J. Am. Chem. Soc. **1992**, *114*, 3445–3455

chromatography on a column of silica gel with petroleum ether elution. A solution of 3-phenoxy[2-^{14}C]propyl bromide (4.1 g, 0.019 mol) in 10 mL of a 33% solution of trimethylamine in ethanol was allowed to stand at room temperature. The product, *N,N,N*-trimethyl-*N*-(3-phenoxy[2-^{14}C]propyl)ammonium bromide, began to precipitate within 1 h. After 24 h, 5.1 g (0.019 mol, 100%) of product was removed, allowed to dry in the air, and converted in 65% yield into [β-^{14}C]allyl phenyl ether by treatment with freshly prepared silver oxide, as described earlier.[15]

Rearrangements and Isotope Measurements. Rearrangement of allyl phenyl ether was carried out at 220 °C. The product, *o*-allylphenol, was isolated and converted into the phenylurethane, which was purified with sublimation for scintillation counting. The details have been given earlier.[3] A sample of the phenylurethane was weighed on a Cahn balance and was dissolved in 10 mL of cocktail (Fischer Biotech ScintiLene BD, No. BP 455-4). The sample was counted 30 times, that is, three times per cycle for 10 cycles. The 2σ was set at 0.5%. Four samples (replicates) from each conversion were weighed, so that each ^{14}C count was eventually from an average of four samples counted as described. Three low conversions and one complete conversion constituted each rearrangement, and two rearrangements were performed. KIE are calculated as described earlier and are listed in Table I.

Acknowledgment. This research was supported by the National Science Foundation, Grants No. 89-19768 and 88-18894.

Registry No. Malonic-*2-^{14}C* acid, 3715-08-0; diethyl malonate-*2-^{14}C*, 5102-68-1; 1,3-dibromopropane-*2-^{14}C*, 139607-00-4; 1-bromo-3-phenoxypropane-*2-^{14}C*, 139607-01-5; *N,N,N*-trimethyl-3-phenoxy-1-propanaminium-*2-^{14}C* bromide, 139607-02-6; 3-phenoxy-1-propene-*2-^{14}C*, 139607-03-7; allyl phenyl ether, 1746-13-0; carbon-14, 14762-75-5.

---

(15) Kupczyk-Subotkowska, L.; Shine, H. J. *J. Labelled Compd. Radiopharm.* **1986**, *24*, 303.

Nature of the Reactive Intermediates from the Iron-Induced Activation of Hydrogen Peroxide: Agents for the Ketonization of Methylenic Carbons, the Monooxygenation of Hydrocarbons, and the Dioxygenation of Arylolefins

Hui-Chan Tung, Chan Kang, and Donald T. Sawyer*

Contribution from the Department of Chemistry, Texas A&M University,
College Station, Texas 77843. *Received November 6, 1991*

Abstract: The reaction efficiencies and product selectivities for a group of ML/HOOH/substrate/solvent systems have been evaluated. The catalysts include $Fe^{II}(PA)_2$, $Fe^{II}(DPA)_2{}^{2-}$, $Fe^{III}Cl_3$, $[Fe^{II}(OPPh_3)_4](ClO_4)_2$, $[Fe^{II}(bpy)_2](ClO_4)_2$, $[Fe^{II}(MeCN)_4](ClO_4)_2$, $[Fe^{II}(O_2bpy)_2](ClO_4)_2$, and $[Co^{II}(bpy)_2](ClO_4)_2$, the solvents include $(py)_2HOAc$, $(MeCN)_4py$, and MeCN, and the substrates include $c\text{-}C_6H_{12}$, $PhCH_3$, $PhCH_2CH_3$, $c\text{-}C_6H_{10}$, and $c\text{-}PhCH{=}CHPh$. When the HOOH/ML ratio is at least 10, all of the complexes catalytically ketonize methylenic carbons and dioxygenate arylolefins. The most effective catalyst systems are $Fe^{II}(PA)_2/py_2(HOAc)$ (e.g., with $c\text{-}C_6H_{12}$ the process is 70% efficient and 95% selective), $Fe^{II}(OPPh_3)_4{}^{2+}/MeCN$, and $Co^{II}(bpy)_2{}^{2+}/(MeCN)_4py$, which activate nucleophilic HOOH via their electrophilicity. The reactive intermediates appear to be $[(PA)_2Fe^{IV}(OH)(OOH)$, **3**], $[(Ph_3PO)_4{}^{2+}Fe^{IV}(OH)(OOH)$, **3′**], and $[(bpy)_2{}^{2+}Co^{IV}(OH)(OOH)$, **3‴**], which are representative of all of the catalysts. These same intermediates also dioxygenate arylolefins. A precursor intermediate [a one-to-one ML/HOOH adduct: e.g., $[(PA)_2{}^{-}Fe^{II}OOH + pyH^+$, **1**]] monooxygenates (oxidizes) hydrocarbons to alcohols and Rpy and reacts with excess HOOH to form species **3**. Although the latter is the favored path for the $Fe^{II}(PA)_2/(py)_2HOAc$ and $Co^{II}(bpy)_2{}^{2+}/(MeCN)_4py$ systems, the monooxygenation path is dominant for the $Fe^{III}Cl_3/MeCN$ and $Fe^{II}(OPPh_3)_4{}^{2+}/MeCN$ systems. In the presence of olefins, species **1** undergoes dehydration to $(PA)_2Fe^{IV}{=}O$, **2**, which transforms them to epoxides. Similar intermediates and reaction paths are observed when *t*-BuOOH is used in place of HOOH. With *t*-BuOOH the reactivity of species **1** with substrate (RH) becomes dominant to give Rpy or ROH, and species **3** reacts with methylenic carbons to give mixtures of ROOBu-*t* and ketone. Evaluation of the kinetic isotope effect with cyclohexane and toluene for the full range of catalysts and solvents gives k_H/k_D values of 2.4 to >10 for the ketonization of $c\text{-}C_6H_{12}$, 2.7–4.7 for $PhCH_3$, 1.4–2.9 for the hydroxylation process, and 1.7 for the Rpy production process $[Fe^{II}(PA)_2/(py)_2HOAc/c\text{-}C_6H_{12}]$.

During the past decade, several reports have discussed the iron-induced activation of hydrogen peroxide (HOOH) for the catalytic and selective oxygenation of hydrocarbon substrates via non-Fenton-chemistry pathways. The transformations have included the following: (a) the ketonization of methylenic carbons [e.g., $c\text{-}C_6H_{12} \rightarrow c\text{-}C_6H_{10}(O)$] with (i) a $Fe^{III}Cl_3/HOOH/(py)_4HOAc$ system,[1] (ii) a $Fe^{II}(PA)_2/HOOH/(py)_2HOAc$ system (PA, anion of picolinic acid),[2] and (iii) a $Co^{II}(bpy)_2{}^{2+}/HOOH/(MeCN)_4py$ system;[3] (b) the dioxygenation of arylolefins and acetylenes with (i) a $Fe^{II}(MeCN)_4{}^{2+}/HOOH/MeCN$ system,[4,5] (ii) a $Fe^{III}Cl_3/HOOH/MeCN$ system,[6] (iii) a $Fe^{II}(PA)_2/HOOH/(py)_2HOAc$ system,[2] and (iv) a $Co^{II}(bpy)_2{}^{2+}/HOOH/(MeCN)_4py$ system;[3] and (c) the epoxidation of olefins with the preceding four systems.[2–6] Although there is good evidence that the reactive intermediate for olefin epoxidation is a ferryl ($L_xFe^{IV}{=}O$) or perferryl ($L_yFe^{V}{=}O$) species,[7] there is complete discord as to the formulation(s) of the activated complex for the (a) ketonization and (b) dioxygenation processes. The latest propositions[8,9] of the Barton group envision the interaction of a binuclear (μ-oxo)[iron(III)] complex with HOOH to give $[L_nFe^{III}OFe^{V}(O)L_n]$, which selectively reacts with R_2CH_2 to form an iron–carbon σ-bond (intermediate **A**). The latter is believed to react with a second HOOH to form an intermediate $[L_nFe^{III}OFe^{V}(OOH)(CHR_2)]$ that collapses to give $R_2CH(OOH)$ and ketone. They also suggest that some of intermediate **A** re-

---

(1) Barton, D. H. R.; Halley, F.; Ozbalik, N.; Young, E. *New J. Chem.* **1989**, *13*, 177.

(2) Sheu, C.; Richert, S. A.; Cofré, P.; Ross, B., Jr.; Sobkowiak, A.; Sawyer, D. T.; Kanofsky, J. R. *J. Am. Chem. Soc.* **1990**, *112*, 1936–1942.

(3) Tung, H.-C.; Sawyer, D. T. *J. Am. Chem. Soc.* **1990**, *112*, 8214–8215.

(4) Sugimoto, H.; Sawyer, D. T. *J. Am. Chem. Soc.* **1984**, *106*, 4283–4285.

(5) Sugimoto, H.; Sawyer, D. T. *J. Am. Chem. Soc.* **1985**, *107*, 5712–5716.

(6) Sugimoto, H.; Sawyer, D. T. *J. Org. Chem.* **1985**, *50*, 1784–1786.

(7) Sugimoto, H.; Tung, H.-C.; Sawyer, D. T. *J. Am. Chem. Soc.* **1988**, *110*, 2465.

(8) Barton, D. H. R.; Doller, D.; Balavoine, G. *J. Chem. Soc., Chem. Commun.* **1990**, 1787.

(9) Barton, D. H. R.; Doller, D.; Ozbalik, N.; Balavoine, G. *Proc. Natl. Acad. Sci. U.S.A.* **1990**, *87*, 3401.

0002-7863/92/1514-3445\$03.00/0

arranges to intermediate **B** [$\mathrm{L}_n\mathrm{Fe}^{\mathrm{III}}\mathrm{OFe}^{\mathrm{III}}(\mathrm{OCHR}_2)\mathrm{L}_n$] to account for the 5–20% yield of alcohol.

In contrast, our group[2] has proposed the formation of a single reactive intermediate for the ketonization process

$$\mathrm{(PA)_2Fe^{III}OFe^{III}(PA)_2} \xrightarrow{\mathrm{2HOOH}} \mathrm{(PA)_2Fe^{IV}(\mu\text{-}O)(\mu\text{-}OO)Fe^{IV}(PA)_2}$$

Several alternative formulations have been suggested on the basis of subsequent experiments: [$\mathrm{(PA)_2Fe^{III}OOFe^{III}(PA)_2}$],[10] [$\mathrm{(PA)_2Fe^{IV}(\mu\text{-}O)_2Fe^{IV}(PA)_2}$],[11] and [$\mathrm{Cl_3Fe^{V}(O_2)}$].[11] We have further proposed[2,10,11] that the reactive intermediate for ketonization also dioxygenates arylolefins and acetylenes and that independent 1:1 iron–HOOH adducts are the reactive intermediates for alcohol production and the epoxidation of olefins.

Although significant experimental support is given for the various formulations of the reactive intermediate for the selective ketonization of methylenic carbons, all have serious limitations. For example, the C–H bond of cyclohexane (ΔH_{DBE}, 95.5 kcal mol^{-1})[12] must be broken by the reactive intermediate in the initial step of the ketonization process. Although hydroxyl radical ($\mathrm{HO^{\bullet}}$; HO–H, $-\Delta G_{\mathrm{BF}} = 111$ kcal mol^{-1}) and atomic oxygen ($\mathrm{{}^{\bullet}O^{\bullet}}$: $\mathrm{{}^{\bullet}O{-}H}$, $-\Delta G_{\mathrm{BF}} = 98$ kcal mol^{-1}) possess sufficient energy,[13] they are not a part of any of the proposed reactive intermediates [$\mathrm{L}_n\mathrm{Fe^{V}{=}O}$, $\mathrm{L}_n\mathrm{Fe^{III}OFe^{V}(O)L}_n$, $\mathrm{(PA)_2Fe^{III}OOFe^{III}(PA)_2}$, $\mathrm{(PA)_2Fe^{IV}(\mu\text{-}O)_2Fe^{IV}(PA)_2}$]. Furthermore, the most highly reactive of the oxene adducts [$\mathrm{(Por^{\bullet +})Fe^{IV}{=}O}$] does not react with saturated hydrocarbons.[7] For such substrates the only generally reactive oxy radical is $\mathrm{HO^{\bullet}}$ which, when generated by the Fenton process, has relative reaction probabilities per C–H bond for primary, secondary, and tertiary carbon centers, $k_{1°}/k_{2°}/k_{3°}$, in aqueous media of 0.10/0.48/1.0 and in $\mathrm{(pyridine)_2}$acetic acid solvent of 0.07/0.44/1.0, respectively.[14] The respective C–H bond energies are 100, 96, and 93 kcal mol^{-1}.[12]

The fundamental considerations for any viable reactive intermediate for the ketonization of methylenic carbons and for the mechanism of its formation from HOOH include the following.

(a) A catalytic process requires *two* oxygen atoms per substrate transformation {$\mathrm{2HOOH \rightarrow 2[O] + 2H_2O}$; $2(t\text{-BuOOH}) \rightarrow 2[\mathrm{O}] + 2(t\text{-BuOH})$; $\mathrm{O_2 \rightarrow 2[O]}$}.

(b) The path to the formation of ketone does not produce an alcohol intermediate.[1–3,8–11]

(c) The reactive intermediate must have the thermodynamic and mechanistic wherewithal to break a 95.5 kcal mol^{-1} C–H bond (ΔH_{DBE} for c-$\mathrm{C_6H_{12}}$).[12]

(d) A closely similar reactive intermediate (to that from HOOH) is formed by $\mathrm{O_2}$ in combination with $\mathrm{Fe(DPA)_2^{2-}}$ (DPA, dianion of 2,6-pyridinedicarboxylic acid).[2,15] However, with $\mathrm{O_2}$ the process is not catalytic and the iron must be reduced and anionic.

(e) The catalytic cycle is independent of the initial oxidation state and form of the iron catalyst [$\mathrm{Fe^{II}(PA)_2}$ is equivalent in catalytic efficiency to $\mathrm{Fe^{III}(PA)_3}$, $\mathrm{Fe^{III}(PA)_2(OAc)}$, and $\mathrm{(PA)_2Fe^{III}OFe^{III}(PA)_2}$].[2]

On the basis of the efficient activation of HOOH by bis(picolinato)iron(II) [$\mathrm{Fe^{II}(PA)_2}$] in $\mathrm{py_2(HOAc)}$[2] and by [$\mathrm{Co^{II}(bpy)_2](ClO_4)_2}$ in $\mathrm{(MeCN)_4py}$[3] for the selective ketonization of methylenic carbons and the dioxygenation of arylolefins, we have undertaken a systematic evaluation of seven iron complexes [$\mathrm{Fe^{II}(PA)_2}$, $\mathrm{Fe^{II}(DPA)_2^{2-}}$, $\mathrm{Fe^{III}Cl_3}$, $\mathrm{Fe^{II}(O_2bpy)_2^{2+}}$, $\mathrm{Fe^{II}(OPPh_3)_4^{2+}}$, $\mathrm{Fe(MeCN)_4^{2+}}$, and $\mathrm{Fe^{II}(bpy)_2^{2+}}$] and $\mathrm{Co^{II}(bpy)_2^{2+}}$ for the activation of HOOH and *t*-BuOOH in three solvent systems [$\mathrm{py_2(HOAc)}$, $\mathrm{(MeCN)_4py}$, and MeCN]. The reaction efficiencies and product profiles have been determined for five hydrocarbon substrates [c-$\mathrm{C_6H_{12}}$, $\mathrm{PhCH_2CH_3}$, $\mathrm{PhCH_3}$, c-$\mathrm{C_6H_{10}}$, and c-PhCH=CHPh]. In addition, the kinetic isotope effects (KIE, $k_{\mathrm{H}}/k_{\mathrm{D}}$) with cyclohexane and toluene have been measured for each catalytic system.

Experimental Section

Equipment. The reaction products were separated and identified with a Hewlett-Packard 5880A series gas chromatograph equipped with an HP-1 capillary column (cross-linked methyl silicone gum phase, 12 m × 0.2 mm i.d.) and by gas chromatography–mass spectrometry (Hewlett-Packard 5790A series gas chromatograph with a mass-selective detector). A Vacuum Atmospheres inert-atmosphere glovebox was used for the storage, preparation, and addition of air-sensitive and water-sensitive reagents.

A three-electrode potentiostat (Bioanalytical Systems Model CV-27) with a Houston Instruments Model 200 XY recorder was used to record the voltammograms. The experiments were conducted in a 15-mL electrochemical cell with a provision to control the presence of oxygen with an argon-purge system. The working electrode was a Bioanalytical Systems glassy-carbon inlay (area, 0.09 cm^2), the auxiliary electrode was a platinum wire, and the reference electrode was a Ag/AgCl wire in an aqueous tetramethylammonium chloride solution that was adjusted to give a potential of 0.00 V vs SCE. The latter was contained in a Pyrex tube with a cracked soft-glass tip, which was placed inside a luggin capillary.[16] A Hewlett-Packard Model 8450A diode-array spectrophotometer was used for the UV–visible measurements.

Chemicals and Reagents. The reagents for the investigations and syntheses were the highest purity commercially available and were used without further purification. Burdick and Jackson "distilled in glass" grade acetonitrile (MeCN, 0.004% $\mathrm{H_2O}$), dimethylformamide (DMF, 0.011% $\mathrm{H_2O}$), pyridine (py, 0.014% $\mathrm{H_2O}$), and glacial acetic acid (HOAc, ACS grade, Fisher) were used as solvents. High-purity argon gas was used to deaerate the solutions. All compounds were dried in vacuo over $\mathrm{CaSO_4}$ for 24 h prior to use. Ferric chloride (anhydrous, 98%), picolinic acid (PAH, 99%), 2,6-pyridinedicarboxylic acid ($\mathrm{DPAH_2}$, 99%), 2,2′-bipyridine (bpy, 99+%), and triphenylphosphine oxide ($\mathrm{OPPh_3}$, 98%) were obtained from Aldrich, hydrogen peroxide (50% $\mathrm{H_2O}$) was obtained from Fisher, and *t*-BuOOH (5.5 M, in 2,2,4-trimethylpentane) was obtained from Aldrich. The organic substrates included cyclohexane (Aldrich, anhydrous 99+%), cyclohexane-d_{12} (Aldrich, 99.5 atom % D), ethyl benzene (Kodak, 99.8%), toluene (Burdick and Jackson, 0.005% $\mathrm{H_2O}$), toluene-d_3 (MSD Isotopes, 99.9 atom % D), cyclohexene (Fisher, 99%), adamantane (Aldrich, 99+%), and *cis*-stilbene (Aldrich, 97%).

Syntheses of $\mathrm{(Me_4N)PA}$ and $\mathrm{(Me_4N)_2DPA}$. Tetramethylammonium picolinate [$\mathrm{(Me_4N)PA}$] and tetramethylammonium dipicolinate [$\mathrm{(Me_4N)_2DPA}$] were prepared by the neutralization of picolinic acid (PAH) and 2,6-pyridinedicarboxylic acid ($\mathrm{DPAH_2}$) with tetramethylammonium hydroxide pentahydrate in aqueous solution. $\mathrm{(Me_4N)PA}$ was recrystallized from acetonitrile and $\mathrm{(Me_4N)_2DPA}$ from 95% MeCN/5% MeOH. The hydroscopic products were stored under vacuum.

2,2′-Bipyridyl 1,1′-Dioxide ($\mathrm{bpyO_2}$). The $\mathrm{bpyO_2}$ ligand was prepared by oxidation of 2,2′-bipyridine with hydrogen peroxide in acetic acid:[17,18] 2,2′-bipyridine (32 g) was placed in a 500-mL three-necked round-bottom flask that contained glacial acetic acid (200 mL). The solution was warmed to 70 °C, and aqueous hydrogen peroxide (50%, 20 mL) was added dropwise with stirring. The solution was stirred for 7 h at 70 °C, additional HOOH (20 mL) was added, and the solution was stirred for 48 h at 70 °C. The resulting solution was evaporated under reduced pressure to give a pale-yellow solid. The resulting compound was recrystallized from MeOH, yield 35.5 g (92%).

[$\mathrm{Fe^{II}(MeCN)_4](ClO_4)_2}$. The [$\mathrm{Fe^{II}(MeCN)_4](ClO_4)_2}$ complex was prepared by multiple recrystallizations of [$\mathrm{Fe^{II}(H_2O)_6](ClO_4)_2}$ from MeCN.

Iron(II) Bis(picolinate) and Iron(III) Bis(dipicolinate) Solutions. Solutions of $\mathrm{Fe^{II}(PA)_2}$ and $\mathrm{Fe^{II}(DPA)_2^{2-}}$ were prepared in situ by mixing [$\mathrm{Fe^{II}(MeCN)_4](ClO_4)_2}$ with stoichiometric ratios of the ligand anion.[19]

Iron(II) Bis(2,2′-bipyridine) and Cobalt(II) Bis(2,2′-bipyridine) Solutions. The $\mathrm{Fe^{II}(bpy)_2^{2+}}$ and $\mathrm{Co^{II}(bpy)_2^{2+}}$ complexes were prepared in situ

---

(10) Sawyer, D. T.; Sheu, C.; Tung, H.-C.; Sobkowiak, A. In *Dioxygen Activation and Homogeneous Catalytic Oxidation*; Simandi, L. I., Ed.; Elsevier: Amsterdam, 1991; pp 285–296.

(11) Sobkowiak, A.; Tung, H.-C.; Sawyer, D. T. In *Progress in Organic Chemistry*; Lippard, S. J., Ed.; John Wiley: New York; Vol. 40, in press.

(12) Lide, D. R., Ed. *CRC Handbook of Chemistry and Physics*, 71st ed.; CRC Press: Boca Raton, FL, 1990; pp 9-86–98.

(13) Sawyer, D. T. *J. Phys. Chem.* **1989**, *93*, 7977.

(14) Sheu, C.; Sobkowiak, A.; Zhang, L.; Ozbalik, N.; Barton, D. H. R.; Sawyer, D. T. *J. Am. Chem. Soc.* **1989**, *111*, 8030–8032.

(15) Sheu, C.; Sobkowiak, A.; Jeon, S.; Sawyer, D. T. *J. Am. Chem. Soc.* **1990**, *112*, 879–881.

(16) Sawyer, D. T.; Roberts, J. L., Jr. *Experimental Electrochemistry for Chemists*; Wiley-Interscience: New York, 1974; p 144.

(17) Nyholm, R. S.; Turco, A. *J. Chem. Soc.* **1962**, 1121–1122.

(18) Matsushita, T.; Spencer, L.; Sawyer, D. T. *Inorg. Chem.* **1988**, *27*, 1167–1173.

(19) Cofré, P.; Richert, S. A.; Sobkowiak, A.; Sawyer, D. T. *Inorg. Chem.* **1990**, *29*, 2645.

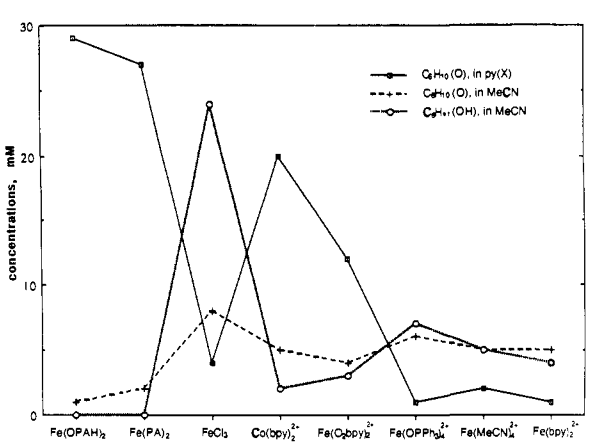

Figure 1. Yields of c-$C_6H_{10}(O)$ and c-$C_6H_{11}OH$ from the combination of 5 mM ML_x, 100 mM HOOH, and 1 M c-C_6H_{12} in (a) $py_2(HOAc)$ [for $Fe^{II}(DPAH)_2$ and $Fe^{II}(PA)_2$], (b) $(MeCN)_4py$ [for other metal complexes], and (c) MeCN. Reaction time: 24 h at 22 ± 1 °C.

by mixing $[Fe^{II}(MeCN)_4](ClO_4)_2$ and $[Co^{II}(MeCN)_4](ClO_4)_2$ in MeCN with stoichiometric ratios of bipyridine.

Iron(II) Tetrakis(triphenylphosphine oxide) and Iron(II) Bis(2,2′-bipyridyl 1,1′-dioxide) Solutions. The $Fe^{II}(OPPh_3)_4^{2+}$ and $Fe^{II}(O_2bpy)_2^{2+}$ complexes were prepared in situ by mixing $[Fe^{II}(MeCN)_4](ClO_4)_2$ in MeCN with stoichiometric ratios of the $OPPh_3$ and O_2bpy ligands.

Methods. The investigations of the HOOH and *t*-BuOOH activation by the iron and cobalt complexes used solutions that contained 1.0 M substrate and 5 mM metal complexes in 7 mL of MeCN, $(MeCN)_4py$, or $py_2(HOAc)$ (mole ratios). Hydrogen peroxide (50%) or *t*-BuOOH (5.5 M) was injected to give 100 mM HOOH(Bu-*t*). After 12 h with constant stirring at room temperature (22 ± 2 °C) under anaerobic conditions, samples of the reaction solutions were injected into a capillary column gas chromatograph for analysis. In some cases, the reaction was quenched with water, and the product solution was extracted with diethyl ether. Product species were characterized by GC-MS. Reference samples were used to confirm product identifications and to produce standard curves for quantitative assays of the product species.

The kinetic isotope effects were determined with a 1:1 cyclohexane/cyclohexane-d_{12} mixture (0.5 M/0.5 M) and a 1:1 toluene/toluene-d_3 mixture as the substrate; the k_H/k_D values were calculated from the product ratios of cyclohexanone/cyclohexanone-d_{10}, cyclohexanol/cyclohexanol-d_{11}, c-C_6H_{11}py/c-C_6D_{11}py, benzaldehyde/benzaldehyde-d_1, and benzyl alcohol/benzyl alcohol-d_2. Similar measurements were made for *t*-BuOOH as the oxidant.

The experiments were designed to be limited by HOOH and *t*-BuOOH in order to (a) evaluate reaction efficiency with respect to oxidant, (b) minimize secondary reactions with the primary products, and (c) minimize catalyst deactivation by product water.

Results

ML/HOOH Systems. The reaction efficiencies and product profiles for the activation of hydrogen peroxide by iron and cobalt complexes for reaction with a variety of hydrocarbon substrates in three solvent matrices are summarized in Table I. The $Fe^{II}(PA)_2$ and $Fe^{II}(DPA)_2^{2-}$ complexes in $py_2(HOAc)$ and the $Co^{II}(bpy)_2^{2+}$ complex in $(MeCN)_4py$ are the most efficient catalysts (58%, 60%, and 40% of HOOH utilized for substrate transformation) for the ketonization of cyclohexane (c-C_6H_{12}), with selectivities for the production of ketone of 87%, 94%, and 98%, respectively. All of the complexes yield some cyclohexanone; with ethylbenzene ($PhCH_2Me$) as the substrate its ketone is the dominant product for each of the catalyst/solvent systems (except $Fe^{III}Cl_3$/MeCN, $Fe^{II}(OPPh_3)_4^{2+}$/MeCN, and $Fe^{II}(O_2bpy)_2^{2+}$/MeCN, which produce mainly hydroxylated-substrate products).

Figure 1 illustrates that the $Fe^{II}(PA)_2$ and $Fe^{II}(DPA)_2^{2-}$ complexes in $py_2(HOAc)$ and the $Co^{II}(bpy)_2^{2+}$ and $Fe^{II}(O_2bpy)_2^{2+}$ complexes in $(MeCN)_4py$ are much more effective ketonization catalysts than when the solvent matrix is pure MeCN. In the latter solvent, $Fe^{III}Cl_3$ is uniquely effective for the activation of HOOH to hydroxylate and chlorinate saturated hydrocarbons and to epoxidize olefins. The $Fe^{II}(OPPh_3)_4^{2+}$, $Fe^{II}(MeCN)_4^{2+}$, and $Fe^{II}(bpy)_2^{2+}$ complexes in MeCN activate HOOH to give almost equal yields of c-$C_6H_{10}(O)$ and c-$C_6H_{11}OH$. With the $Fe^{II}(PA)_2/(py)_2HOAc$/c-C_6H_{12} system the secondary product is c-C_6H_{11}py rather than the alcohol.

The kinetic isotope effects (KIE) for the ketonization and hydroxylation of cyclohexane by the various ML/HOOH/solvent systems have been evaluated via the use of a 0.5 M c-C_6H_{12}/0.5 M c-C_6D_{12} substrate and determination of the ketone and alcohol product ratios (equal to k_H/k_D); the values are in square brackets in the third and fifth columns of data in Table I. The k_H/k_D values for ketonization are larger in pure MeCN (4 to >10) than in the pyridine-containing solvents (2.4–3.4). For the hydroxylation process, the $Fe^{II}(bpy)_2^{2+}$ and $Co^{II}(bpy)_2^{2+}$ catalysts have smaller k_H/k_D values (1.4 and 1.6) than the $Fe^{II}(OPPh_3)_4^{2+}$ and $Fe^{II}(O_2bpy)_2^{2+}$ catalysts (1.9 and 2.1), and $Fe^{III}Cl_3$ has the largest ratio (2.9) (Table I, part C).

When $PhCH_3$ and $PhCH_2CH_3$ are the substrates, the reactive intermediate for substrate hydroxylation in systems with pyridine adds to the aromatic ring rather than the alkyl groups (Table I, parts A and B). With cyclohexene as the substrate the $Co^{II}(bpy)_2^{2+}$ complex in $(MeCN)_4(py)$ is the most effective ketonization catalyst (19 mM 2-cyclohexenone produced). The oxygenation of $PhCH_3$ to PhCH(O) is more efficient in pyridine-containing media than in pure acetonitrile, and $Fe^{II}(MeCN)_4^{2+}$ is the most effective catalyst for the ketonization of $PhCH_2Me$ to PhC(O)Me (21.9 mM) of the group of metal complexes in MeCN.

A measure of the influence of C–H bond energies on reaction probabilities is the ratio of ketone product per methylenic carbon (CH_2) for $PhCH_2Me$ (ΔH_{DBE}, 85 kcal mol^{-1}) and c-C_6H_{12} (ΔH_{DBE}, 95.5 kcal mol^{-1}; $\{R\} = k_{PhCH_2Me}/(k_{c\text{-}C_6H_{12}}/6)$). The values of $\{R\}$ range from 5.1 and 5.0 for $Fe^{II}(PA)_2$ and $Fe^{II}(DPA)_2^{2-}$ to 26.5 for $Fe^{II}(MeCN)_4^{2+}$/MeCN. The three catalysts are almost equally efficient for the ketonization of $PhCH_2Me$, but $Fe^{II}(MeCN)_4^{2+}$ is 5 times less efficient with c-C_6H_{12} (Table I).

Although $Fe^{III}Cl_3$ activates HOOH for the ketonization of c-C_6H_{12} (Table I), it is more efficient in MeCN (KIE, 11) than in $(py)_2HOAc$ (KIE, 2.6). In MeCN its dominant chemistry is hydroxylation and chlorination of substrate.

$Fe^{II}(DPA)_2^{2-}/O_2/(py)_2HOAc$ System. The combination of 32 mM $Fe^{II}(DPA)_2^{2-}$, O_2 (1 atm, 4.1 mM), and 1 M c-C_6H_{12} in $(py)_2HOAc$ yields 4 mM c-$C_6H_{10}(O)$ as the only detectable product, and all of the iron is oxidized to $(DPA)_2^{2-}Fe^{III}OFe^{III}(DPA)_2^{2-}$ in a noncatalytic process. The KIE value for the reactive intermediate with c-C_6H_{12} is 2.6, and its relative reactivity with $PhCH_2Me$/c-C_6H_{12}, $\{R\}$, is 6.0; both parameters are the same (within experimental error) as those for the $Fe^{II}(PA)_2$/HOOH and $Fe^{II}(DPA)_2^{2-}$/HOOH systems. This system also dioxygenates c-PhCH=CHPh to PhCH(O) and catechol to muconic acid.[15] For these solution conditions, $Fe^{II}(PA)_2$ does not activate O_2 and is not auto-oxidized.

ML/*t*-BuOOH Systems. Table II summarizes the reaction efficiencies and product profiles for the same catalyst/substrate/solvent systems (Table I) when 100 mM *t*-BuOOH is used in place of HOOH. With $Fe^{II}(PA)_2$/c-C_6H_{12} the overall oxidation efficiency is almost the same (61% for *t*-BuOOH and 58% for HOOH). However, in place of the production of 27 mM c-$C_6H_{10}(O)$ (KIE, 2.5) and 4 mM c-C_6H_{11}py with HOOH, the products from *t*-BuOOH are 6 mM c-$C_6H_{10}(O)$ (KIE, 7.6), 7 mM c-$C_6H_{11}OOBu$-*t* (KIE, 8.4), 1 mM c-$C_6H_{11}OH$, and 34 mM c-C_6H_{11}py (KIE, 4.6). In contrast, the $Fe^{II}(PA)_2/PhCH_2Me$ system with HOOH is 52% efficient to give 23 mM PhC(O)Me $\{R$, 5.1$\}$ and 5 mM $HOPhCH_2CH_3$, and with *t*-BuOOH it is 82% efficient to give 12 mM PhC(O)Me $\{R$, 12$\}$ and 28 mM PhCH(OOBu-*t*)CH_3 $\{R$, 24$\}$. In general, the KIE values are larger for *t*-BuOOH than those for HOOH.

Within the family of systems and substrates that are summarized in Tables I and II, the most effective for ketonization (or peroxidation) are the following: for c-C_6H_{12}, $Fe^{II}(DPA)_2^{2-}$/HOOH/$(py)_2HOAc$, $Fe^{II}(PA)_2$/HOOH/$(py)_2HOAc$, and $Fe^{II}(bpy)_2^{2+}$/*t*-BuOOH/$(MeCN)_4py$; for $PhCH_2Me$, $Fe^{II}(bpy)_2^{2+}$/*t*-BuOOH/$(MeCN)_4py$ and $Fe^{II}(bpy)_2^{2+}$/*t*-BuOOH/$(py)_2HOAc$; for $PhCH_3$ $Co^{II}(bpy)_2^{2+}$/*t*-BuOOH/MeCN, $Fe^{II}(PA)_2$/*t*-BuOOH/$(py)_2HOAc$, and $Fe^{III}Cl_3$/*t*-BuOOH/$(MeCN)_4py$; for

Table I. Activation of 100 mM HOOH by 5 mM ML_x Complexes for the Oxygenation of 1 M Hydrocarbon Substrates (RH) in $py_2(HOAc)$, $(MeCN)_4py$, and MeCN Solvent[a]

	products, mM (±0.5)													
	$c\text{-}C_6H_{12}$ (95.5 kcal)			$PhCH_2CH_3$ (85 kcal)				$PhCH_3$ (88 kcal)			$c\text{-}C_6H_{10}$ (87 kcal)			
ML_x complex/RH	react.[b] eff., %	$C_6H_{10}(O)$ $[k_H/k_D]$[c]	$C_6H_{11}py$	react.[b] eff., %	$PhC(O)CH_3$ {R}[d]	PhCH-(OH)CH_3	HOPh-CH_2CH_3	react.[b] eff., %	PhCH(O) $[k_H/k_D]$[e]	HOPh-CH_3	react.[b] eff., %	$C_6H_8(O)$	C_6H_9OH	epoxide
						A. $(py)_2(HOAc)$								
$Fe^{II}(PA)_2$	58	27 [2.5]	4	52	23 {5.1}	<1	5	22	6 [3.0]	10	28[f]	13	0	0
$Fe^{II}(DPA)_2^{2-}$	60	29 [2.4]	2	54	24 {5.0}	<1	5	26	7 [2.9]	12	30	13	0	0
$Fe^{II}(DPA)_2^{2-}/O_2$ 32 mM, 1 atm		(4) [2.6]	0		(4) {6.0}				(1)			(1)		
$Fe^{III}Cl_3$	9	4 [2.6]	<1					8	4 [2.7]	<1				
						B. $(MeCN)_4py$								
		$c\text{-}C_6H_{11}OH$, $[k_H/k_D]$[g]												
$Co^{II}(bpy)_2^{2+}$	40	20 [2.9]	0	41	20 {6.0}	0	1	20	7 [2.7]	6	44	19	4	2
$Co^{II}L_2^{2+}/HOOH$ 20 mM, 200 mM	(62)	(61)	(1)	(36)	(30) {2.9}	(0)	(11)	(29)	(20)	(17)	(56)	(50)	(3)	(8)
$Fe^{II}(O_2bpy)_2^{2+}$	24	12 [3.4]	<1	29	14 {7.0}	<1	1	11	4 [2.9]	3	19	9	<1	<1
$Fe^{III}Cl_3$	2	1	<1											
						C. MeCN								
							$PhCH_2CH_2OH$			$PhCH_2OH$				
$Fe^{III}Cl_3$	40	8 [11]	24[h] [2.9]	59	15 {10.5}	11	20[h]	24	5 [3.3]	5[h] (3)[i]	41	5	18[h]	9
$Fe^{II}(OPPh_3)_4^{2+}$	20	6 [>10]	7 [1.9]	35	6 {6.0}	21	2	13	5 [4.7]	2 (1)[j]	19[f]	3	2	0
$Fe^{II}(MeCN)_4^{2+}$	16	5 [>10]	5 [1.8]	42	22 {26.5}	0	2	12	5 [4.1]	2	9	3	<1	0
$Fe^{II}(bpy)_2^{2+}$	14	5 [4]	4 [1.4]	27	14 {15.6}	0	0 (1)[k]	9	3 [3.4]	1 (2)[j]	18	4	0	9
$Fe^{II}(O_2bpy)_2^{2+}$	11	4 [6]	3 [2.1]	28	6 {9.0}	15	0 (1)[k]	10	3 [4.4]	2 (2)[j]	25	5	14	0
$Co^{II}(bpy)_2^{2+}$	10	5 [4]	0	27	13 {15.6}	0	<1 (1)[k]	14	4 [3.3]	<1 (5)[j]	34	10	12	1
$Co^{II}L_2^{2+}/HOOH$ 20 mM, 200 mM	(14)	(14)									(12)	(30)		

---

[a] Substrate and ML_x combined in 3.5 mL of solvent, followed by the slow addition of 25 μL of 17.6 M HOOH (50% in H_2O) to give 100 mM HOOH. Reaction time and temperature: 4–6 h at 22 ± 2 °C. [b] 100% represents one substrate oxygenation per two HOOH molecules added for carbonyl formation and per one HOOH for alcohol and $c\text{-}C_6H_{11}py$ formation; the remainder of the HOOH was unreacted or consumed via slow O_2 evolution. [c] The product ratios of $c\text{-}C_6H_{10}(O)/c\text{-}C_6D_{10}(O)$, ±10%. [d] $\{R\} = [k_{PhCH_2Me}/(k_{c\text{-}C_6H_{12}}/6)]$, relative reactivity per (CH_2) for $PhCH_2Me$ vs $c\text{-}C_6H_{12}$. [e] The product ratios of PhCH(O)/PhCD(O) from $PhCH_3/PhCD_3$, ±10%. [f] With 5 mM $Fe^{II}(PA)_2$ and 100 mM t-BuOOH the efficiency is 64% to give 2 mM $c\text{-}C_6H_8(O)$, 21 mM $c\text{-}C_6H_9OOBu$, and 9 mM $(c\text{-}C_6H_9)_2$. With 5 mM $Co^{II}(bpy)_2^{2+}$, 100 mM t-BuOOH, and $(MeCN)_4py$ the efficiency is 66% to give 29 mM $c\text{-}C_6H_9OOBu$ and 5 mM $(c\text{-}C_6H_9)_2$. With 5 mM $Fe^{II}(OPPh_3)_4^{2+}$ and 100 mM t-BuOOH the efficiency is 68% to give 32 mM $c\text{-}C_6H_9OOBu$ and 3 mM $c\text{-}C_6H_9OH$. [g] The product ratios of $c\text{-}C_6H_{11}OH/c\text{-}C_6D_{11}OH$, ±10% error. [h] 50–75% RCl. [i] PhC(O)OH. [j] $HOPhCH_3$. [k] $HOPhCH_2CH_3$.

Table II. Activation of 100 mM *t*-BuOOH by 5 mM ML_x Complexes for the Oxygenation of 1 M Hydrocarbon Substrates (RH) in $(py)_2HOAc$, $(MeCN)_4py$, and MeCN Solvents[a]

	products, mM (±0.5)											
	$c\text{-}C_6H_{12}$					$PhCH_2CH_3$				$PhCH_3$		
ML_x complex/RH	react.[b] eff., %	$C_6H_{10}(O)$ $[k_H/k_D]^c$	ROOBu $[k_H/k_D]^c$	ROH $[k_H/k_D]^c$	Rpy $[k_H/k_D]^c$	react.[b] eff., %	$PhC(O)CH_3$ $\{R\}^d$	$PhCH(OOBu)CH_3$ $\{R\}^d$	$PhCH(OH)CH_3$	react.[b] eff., %	PhCH(O) $[k_H/k_D]^c$	ROOBu $[k_H/k_D]^c$
$Fe^{II}(PA)_2/(py)_2HOAc$	61	6 [7.6]	7 [8.4]	1	34 [4.6]	82	12 {12.0}	28 {24.0}	0	39	7 [5.3]	12 [6.0]
$Fe^{III}Cl_3/MeCN$	54	16 [>10]	4 [5.8]	14^e [4.3]		81	10 {3.7}	9 {6.0}	43^e	30	14 [4.8]	1 [>10]
$Fe^{III}Cl_3/(MeCN)_4py$	59	17	10	6^e	0	87	7 {2.5}	31 {18.6}	13^e	39	6	13
$Fe^{III}Cl_3/(py)_2HOAc$	23	6	2	0	9	50	9 {9.0}	13 {39.0}	5^e	21	3 [>10]	8 [>10]
$Fe^{II}(OPPh_3)_4^{2+}/MeCN$	44	13 [10.2]	9 [6.4]	2 [5.2]		79	5 {2.3}	25 {16.7}	20	31	12 [5.3]	3 [>10]
$Fe^{II}(OPPh_3)_4^{2+}/(MeCN)_4py$	48	7	12	1	9	66	17 {14.6}	16 {8.0}	0	32	7	9
$Fe^{II}(MeCN)_4^{2+}/MeCN$	43	15 [>10]	6 [6.0]	1 [5.6]		83	7 {2.8}	28 {28.0}	14	28	12 [53]	2 [>10]
$Fe^{II}(bpy)_2^{2+}/MeCN$	40	15 [>10]	4 [5.4]	1 [4.8]		69	7 {2.8}	6 {9.0}	42	30	13 [4.5]	2 [>10]
$Fe^{II}(bpy)_2^{2+}/(MeCN)_4py$	46	10	11	2	3	83	19 {11.4}	22 {12.0}	0	32	8	8
$Co^{II}(bpy)_2^{2+}/MeCN$	18	5 [9.6]	3 [8.7]	3 [6.3]		72	7 {8.4}	29 {58.0}	0	38	5 [10.2]	15 [>10]
$Co^{II}(bpy)_2^{2+}/(MeCN)_4py$	2	0	1	0		37	6	12 {72.0}	0	7	0	4

[a] Substrate and ML_x combined in 3.5 mL of solvent, followed by the slow addition of 350 μmol of *t*-BuOOH. Reaction time and temperature: 4–6 h at 22 ± 2 °C. [b] 100% represents one substrate (RH) oxygenation per two *t*-BuOOH molecules for carbonyl and *t*-BuOOR formation and per one *t*-BuOOH for alcohol and pyR formation. [c] Product ratios [e.g., $c\text{-}C_6H_{10}(O)/c\text{-}C_6D_{10}(O)$], ±10%. [d] $\{R\} = [k_{PhCH_2Me}/(k_{c\text{-}C_6H_{12}}/6)]$, relative reactivity per (CH_2) for $PhCH_2Me$ vs $c\text{-}C_6H_{12}$. [e] 50–85% RCl.

Table III. Product Profiles for the Combination of $Fe^{II}(PA)_2$ and $(PA)_2Fe^{III}OFe^{III}(PA)_2$ with HOOH (or *t*-BuOOH) in the Presence of 1 M $c\text{-}C_6H_{12}$ in $(py)_2HOAc$[a]

reaction conditions		reaction[b] efficiency, % (±4)	products, mM (±0.5)					
			$c\text{-}C_6H_{10}(O)$	$c\text{-}C_6H_{11}OH$	$(c\text{-}C_6H_{11})py$	$(c\text{-}C_6H_{11})_2$	$PhSe(c\text{-}C_6H_{11})$	PhSe(py)
			A. $Fe^{II}(PA)_2$					
$[Fe^{II}(PA)_2]$	[HOOH]							
3.3 mM	56 mM	72	20	1	0	0		
9 mM	9 mM	58	1.3	0	2.4	0.1		
19 mM	19 mM	49	1.1	0	5.8 [1.7]^c	0.7		
19 mM	19 mM (10 mM PhSeSePh)	100	0.6	0	0	0	17	0.7
20 mM	20 mM *t*-BuOOH	92	0.5	0	16	0.7		
20 mM	20 mM *t*-BuOOH (10 mM PhSeSePh)	25	0	0	0	0	4.5	0.5
		B. 10 mM $(PA)Fe^{III}OFe^{III}(PA)_2$ and 10 mM HOOH [or *m*-ClPhC(O)OOH]						
$c\text{-}C_6H_{12}$ (1 M)		60 [0]	4.0	0	0	0		
c-PhCH=CHPh (0.6 M)		55 [0]	5.6 [PhCH(O)], [0.6 mM PhC(O)C(O)Ph]					

[a] Substrate and $Fe^{II}(PA)_2$ or $(PA)_2Fe^{III}OFe^{III}(PA)_2$ were combined in 3.5 mL of $(py)_2HOAc$ solvent, followed by the slow addition (1–2 min) of 2–13 μL of 17.3 M HOOH (49%) in H_2O to give 9–56 mM HOOH. [b] 100% represents one product species per two HOOH [except for the production of $PhSe(c\text{-}C_6H_{11})$, $c\text{-}C_6H_{11}OH$, and $c\text{-}C_6H_{11}py$, which require one HOOH]. [c] Product ratio of $c\text{-}C_6H_{11}py/c\text{-}C_6D_{11}py$, ±10%.

cyclohexene ($c\text{-}C_6H_{10}$), $Fe^{II}(OPPh_3)_4^{2+}/t\text{-}BuOOH/MeCN$, $Co^{II}(bpy)_2^{2+}/t\text{-}BuOOH/(MeCN)_4py$, and $Fe^{II}(PA)_2/t\text{-}BuOOH/(py)_2HOAc$.

Variation of $Fe^{II}(PA)_2$/HOOH Mole Ratio. Because the $Fe^{II}(PA)_2/(py)_2HOAc/c\text{-}C_6H_{12}$ system was the most impressive of the catalyzed ketonizations, it has been subjected to a series of studies to gain insight into the reaction paths and the reactive intermediates. Table IIIA summarizes the product profiles for $c\text{-}C_6H_{12}$ when the $Fe^{II}(PA)_2$/HOOH mole ratio is varied from 3.3 mM/56 mM (92% efficient and 95% selective to produce ketone) to 19 mM/19 mM (49% efficient and 14% selective to produce ketone; the dominant product is $c\text{-}C_6H_{11}py$ (76%)). For the latter condition, the presence of a radical trap (PhSeSePh)[14] causes the process to become 100% efficent to give $c\text{-}C_6H_{11}SePh$ (93%), $c\text{-}C_6H_{10}(O)$ (3%), and PhSe(py) (4%). In contrast, the combination of 20 mM $Fe^{II}(PA)_2$, 20 mM *t*-BuOOH, and 1 M $c\text{-}C_6H_{12}$ reacts with 92% efficiency to give $c\text{-}C_6H_{11}py$ (93%; a yield of 16 mM from 20 mM *t*-BuOOH indicates a 1:1 reaction stoichiometry), $c\text{-}C_6H_{10}(O)$ (3%), and $(c\text{-}C_6H_{11})_2$ (4%). With PhSeSePh present in the latter system, the efficiency drops to 25% to give $c\text{-}C_6H_{11}SePh$ (90%) and PhSe(py) (10%).

The results from the one-to-one combination of $(PA)_2Fe^{III}OFe^{III}(PA)_2$ and HOOH [or *m*-ClPhC(O)OOH] with $c\text{-}C_6H_{12}$ and c-PhCH=CHPh are summarized in Table III, part B. The 100% selectivity for production of $c\text{-}C_6H_{10}(O)$ is impressive and is consistent with a unique reactive intermediate (the same as from the $Fe^{II}(PA)_2$/HOOH system) for the ketonization of methylenic carbons and dioxygenation of arylolefins. The absence of any product when *m*-ClPhC(O)OOH is the source of oxygen is compelling evidence against two proposed reactive intermediates, $(PA)_2Fe^{III}OOFe^{III}(PA)_2$ and $(PA)_2Fe^{IV}(\mu\text{-}O)_2Fe^{IV}(PA)_2$.[2,10,11]

Reaction Dynamics. The rate of formation of $c\text{-}C_6H_{10}(O)$ from $c\text{-}C_6H_{12}$ (0.1–1.0 M) by the $Fe^{II}(PA)_2$ (1–20 mM)/HOOH (10–200 mM)/$(py)_2HOAc$ system conforms to a rate law that is first-order each in the concentration of $Fe^{II}(PA)_2$, HOOH, and $c\text{-}C_6H_{12}$: on the basis of the initial rates of reaction, the apparent rate constant, k_{ox}, is $(5 \pm 3) \times 10^{-2}$ M^{-2} s^{-1} at 25 °C [$d[c\text{-}C_6H_{10}(O)]/dt = k_{ox}[Fe^{II}(PA)_2][HOOH][c\text{-}C_6H_{12}]$].

Adamantane. The reaction efficiencies and product profiles for the $Fe^{II}(PA)_2$/HOOH (and *t*-BuOOH) system and adamantane ($C_{10}H_{16}$, with six $>CH_2$ groups and four $\geqslant CH$ groups) are summarized in Table IV. With HOOH the reaction efficiency is only 30% and ketonization is favored, but substantial yields of tertiary $C_{10}H_{15}py$ are produced. In contrast, *t*-BuOOH reacts with 72% efficiency, and the dominant products are $1\text{-}C_{10}H_{15}\text{-}2\text{-}py$ and $1\text{-}C_{10}H_{15}\text{-}4\text{-}py$. The yield of ketone is almost the same as with

Table IV. Product Profiles for the Combination of 5 mM $Fe^{II}(PA)_2$, 100 mM HOOH (or *t*-BuOOH), and 0.1 M Adamantane ($C_{10}H_{16}$) in $(py)_2HOAc$

oxidant	react.[a] eff., % (±4)	products, mM (±0.5)				ratio[b]
		$C_{10}H_{14}(O)$	1-$C_{10}H_{15}OH$	1-$C_{10}H_{15}$-2-py	1-$C_{10}H_{15}$-4-py	
HOOH	30	9.0	<0.5	8.1	3.7	[2.2]
t-BuOOH	72	8.4	0.5	32.3	22.4	[1.4]

[a] 100% represents one substrate oxygenation per two HOOH (or *t*-BuOOH) molecules for adamantanone formation and per one HOOH for alcohol and Rpy formation. [b] Relative reaction probability with two and four carbons of pyridine. With 3 mM $Fe^{II}(PA)_2$/56 mM HOOH the ratio is 1.8; ref 2.

Table V. Reactivity of 5 mM ML_x/100 mM HOOH/$py_2(HOAc)$, $(MeCN)_4py$, or MeCN Systems with 0.6 M c-PhCH=CHPh (Results for 100 mM *t*-BuOOH)

catalyst	react. eff., % (±1)	products, mM (±1.0)		
		PhCH(O)	PhC(O)C(O)Ph	epoxide
A. $py_2(HOAc)$				
$Fe^{II}(PA)_2$[b]	40 (18)[c]	31 (15)[c]	3 (1)[c]	0.1
$Fe^{II}(DPAH)_2$	39 (0.1)	33 (0.1)	2	
[32 mM $Fe^{II}(DPAH)_2$ O_2, 1 atm]	[5]	[3]		
$Fe^{III}Cl_3$	23 (3)	23 (3)		0.1
B. $(MeCN)_4py$				
$Co^{II}(bpy)_2^{2+}$	41 (0.5)	35 (0.5)	2	
[20 mM/200 mM $Co^{II}L_2^{2+}$/HOOH]	[46]	[87]		[4]
$Fe^{II}(O_2bpy)_2^{2+}$	28 (10)	25 (7)	1 (1)	
$Fe^{III}Cl_3$	3 (14)	3 (14)	(0.1)	0.3
C. MeCN[d]				
$Fe^{III}Cl_3$	52 (53)	36 (41)	3 (3)	7 (3)
[100 mM]	[46]	[28]	[2]	[0.1], [6 mM dioxane][e]
$Fe^{II}(OPPh_3)_4^{2+}$	60 (32)	29 (24)	7 (2)	[5 mM PhC(O)OH] (2)
$Fe^{II}(MeCN)_4^{2+}$	55 (30)	36 (22)	6 (2)	1 (2)
$Fe^{II}(bpy)_2^{2+}$	38 (19)	33 (14)	1 (1)	2 (2)
$Co^{II}(bpy)_2^{2+}$	14 (10)	14 (6)	(0.4)	0 (3)

[a] 100% represents one substrate dioxygenation per two HOOH (or *t*-BuOOH) molecules to give two PhCH(O). Production of PhC(O)C(O)Ph requires three HOOH molecules, and production of epoxide requires one HOOH molecule. [b] With 3.5 mM $Fe^{II}(PA)_2$ and 56 mM HOOH the reaction efficiency is 36% to give 15 mM PhCH(O) and 5 mM epoxide. [c] Results for 100 mM *t*-BuOOH in parentheses. [d] The combination of ML/HOOH/c-Ph$\overline{\mathrm{CHC(O)}}$HPh [5 mM/100 mM/100 mM] in MeCN produces some PhCH(O): $Fe^{II}(MeCN)_4^{2+}$, 10.6 mM; $Fe^{II}(OPPh_3)_4^{2+}$, 10.0 mM; $Fe^{II}(O_2bpy)_2^{2+}$, 4.8 mM; $Fe^{II}(bpy)_2^{2+}$, 8.0 mM; and $Fe^{III}Cl_3$, 9.7 mM. However, PhC(O)C(O)Ph is unreactive. [e] Dimer product from 12 mM epoxide; ref 6.

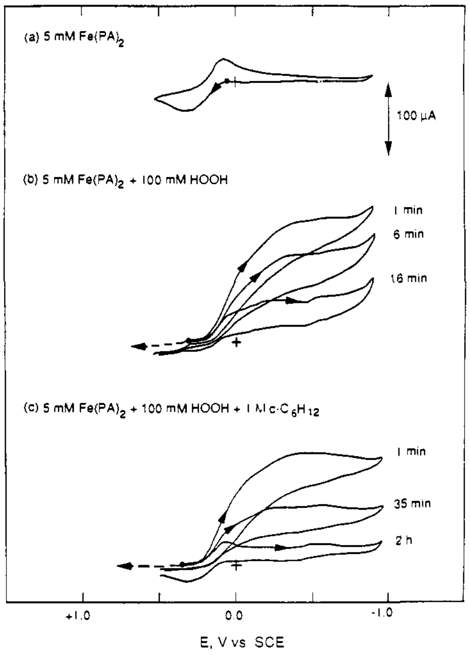

Figure 2. Cyclic voltammograms at a glassy-carbon electrode (area 0.09 cm^2) in $(py)_2HOAc$ [0.1 M tetraethylammonium perchlorate] for (a) $Fe^{II}(PA)_2$, (b) $Fe^{II}(PA)_2$ in the presence of excess HOOH, and (c) $Fe^{II}(PA)_2$ in the presence of excess HOOH and 1 M c-C_6H_{12}. The duration of the reaction for solutions b and c is indicated on the voltammograms. Scan rate: 0.1 V s^{-1}.

HOOH, but no $C_{10}H_{15}OOBu$-*t* is detected.

Dioxygenation of c-PhCH=CHPh. Table V summarizes the reaction efficiencies and product profiles for the various ML_x/HOOH (or *t*-BuOOH)/solvent systems in combination with c-PhCH=CHPh. Although a dioxygenation path to give PhCH(O) is dominant for all systems, the $Fe^{III}Cl_3$/MeCN system produces substantial epoxide, and the $Fe^{II}(OPPh_3)_4^{2+}$/MeCN and $Fe^{II}(MeCN)_4^{2+}$/MeCN systems produce some PhC(O)C(O)Ph [probably in two steps: c-PhCH=CHPh → PhC≡CPh → PhC(O)C(O)Ph]. With most systems the dioxygenation efficiencies are 2 or 3 times greater for HOOH relative to *t*-BuOOH. However, with the $Fe^{III}Cl_3$/MeCN and $Fe^{II}(OPPh_3)_4^{2+}$/MeCN systems the yields of PhCH(O) are essentially equivalent. The combination of 5 mM $Fe^{II}(PA)_2$ with 100 mM HOOH in $(py)_2HOAc$ is 40% efficient to give 91% PhCH(O), 9% PhC(O)C(O)Ph, and 0.3% epoxide; in contrast, 3.5 mM $Fe^{II}(PA)_2$/56 mM HOOH is 36% efficient to give 75% PhCH(O) and 25% epoxide.[2]

Characterization of the Reactive Intermediate for the $Fe^{II}(PA)_2$/HOOH/c-C_6H_{12}/$(py)_2HOAc$ System. Figure 2 illustrates the cyclic voltammograms in $(py)_2HOAc$ for $Fe^{II}(PA)_2$, $Fe^{II}(PA)_2$ plus excess HOOH, and $Fe^{II}(PA)_2$ plus excess HOOH and c-C_6H_{12}. The $Fe^{II}(PA)_2$ complex in the absence of HOOH is oxidized at +0.3 V vs SCE by a 1-electron process to give $(PA)_2Fe^{III}(OAc)$, which is reduced at +0.1 V vs SCE. With 100 mM HOOH present, the rest potential is shifted to +0.4 V and there is a total absence of reduced iron. An initial negative voltage scan (within 1 min of mixing) gives a broad reduction peak with a current that is equivalent to 2–6 electrons per iron (at a scan rate of 0.8 V s^{-1} the current is equivalent to about 2 electrons per iron, and at 0.010 V s^{-1} it is about 6 electrons per iron). After 16 min, the peak current has decayed by about 75% and is equivalent to 2 electrons per iron. If 1 M c-C_6H_{12} and 100 mM HOOH are combined with 5 mM $Fe^{II}(PA)_2$, the initial negative scan after 1 min of reaction time gives a reduction peak that is essentially the same as that when c-C_6H_{12} is absent (Figure 2c). However, the rate of decay of the peak current is 4–5 times slower with c-C_6H_{12} present. After 12 h of reaction time, the 5 mM $Fe^{II}(PA)_2$/100 mM HOOH system yields a cyclic voltammogram with only reduction peaks at −0.65 V vs SCE [characteristic of $(PA)_2Fe^{III}(\mu\text{-}OH)_2Fe^{III}(PA)_2$][19] and −0.85 V vs SCE [characteristic of $(PA)_2Fe^{III}OFe^{III}(PA)_2$].[19] When c-$C_6H_{12}$ is present and after 24 h of reaction time, the solution yields a cyclic voltammogram with an anodic peak at +0.3 V vs SCE that indicates that more than half of the iron is $Fe^{II}(PA)_2$. A pattern of cyclic voltammograms similar to that for the $Fe^{II}(PA)_2$/HOOH system (Figure 2b) results when 100 mM *t*-BuOOH is used in place of HOOH, but the decay rate is about 36 times slower in the absence of c-C_6H_{12} and 15 times slower in its presence.

The cyclic voltammogram for the product solution from the combination of 19 mM $Fe^{II}(PA)_2$, 19 mM HOOH, and 1 M c-C_6H_{12} (Table III, part A, c-C_6H_{11}py dominant product) indicates that more than half of the iron remains as $Fe^{II}(PA)_2$. However, when 10 mM PhSeSePh is present, the electrochemistry of the product solution (Table III, part A, c-C_6H_{11}SePh dominant product) indicates that all of the iron is in the oxidized state [$(PA)_2Fe^{III}(OAc)$].

The UV–visible absorption spectra in $(py)_2HOAc$ for $Fe^{II}(PA)_2$ and for the $Fe^{II}(PA)_2$/HOOH and Fe^{II}/HOOH/c-C_6H_{12} combinations as a functioin of time are illustrated in Figure 3. Addition of HOOH causes the absorption band for $Fe^{II}(PA)_2$ (λ_{max}, 402 nm) to immediately disappear to give an absorption shoulder at 310 nm (pale brown solution), which becomes obscured after 20 min by the emergence of a new band at 380 nm (dark brown solution). When 1 M c-C_6H_{12} is present, the same sequence of spectral changes occur, but is 4 times slower. After 24 h, the latter solution has a spectrum that indicates that more than half of the iron is in the reduced state [$Fe^{II}(PA)_2$; λ_{max}, 402 nm].

A similar set of electrochemical and spectral changes occurs in MeCN for the 5 mM $Fe^{II}(OPPh_3)_4^{2+}$/100 mM HOOH and 5 mM $Fe^{II}(OPPh_3)_4^{2+}$/100 mM HOOH/1 M c-C_6H_{12} systems. The $Fe^{II}(OPPh_3)_4^{2+}$ complex (5 mM) only absorbs below 280 nm (λ_{max}, 266 nm), but addition of 100 mM HOOH causes the slow emergence of a shoulder at 292 nm (half-maximum absorbance in 35 min). If 1 M c-C_6H_{12} is present, the same shoulder emerges with a half-maximum time of about 1 min, but the maximum absorbance is only 0.8 of that for the system without c-C_6H_{12}. Immediately after preparation, this system exhibits a multielectron reduction at +0.1 V vs SCE (the II/III redox couple for $Fe^{II}(OPPh_3)_4^{2+}$ is at +1.1 V vs SCE). With the $Fe^{III}Cl_3$/HOOH/MeCN system a new reduction peak appears at +0.15 V vs SCE; when the solvent is $(py)_2HOAc$ the new peak occurs at −0.3 V. In contrast, the $Co^{II}(bpy)_2^{2+}$/HOOH/$(MeCN)_4$py system gives a small new peak (0.25 e^-) at 0.0 V, and there is essentially no change with time in the absence of substrate.

Discussions and Conclusions

The results that are summarized in Tables I–V indicate that this group of metal complexes activate HOOH and *t*-BuOOH to transform methylenic carbons to ketones and/or ROOBu-*t* and alcohols or Rpy (when pyridine is present in the solvent). The efficiencies in utilization of HOOH and the selectivities in product formation are a function of the metal complex, the hydrocarbon substrate, and the solvent matrix (Figure 1, Tables I and III). The kinetic isotope effects (KIE) for c-C_6H_{12} and $PhCH_3$ with all systems are larger than those for HO• (for c-C_6H_{12} in H_2O; KIE, 1.1).[20] This and the reaction stoichiometries of Tables I and III as well as the catalytic cycles preclude (a) free hydroxyl radical as a reactive intermediate and (b) the Fenton process (which is noncatalytic with one HO• formed per one 1:1 iron(II)/HOOH) as a component of the reaction pathways for these systems.

Primary Step: Nucleophilic Addition by HOOH(Bu-*t*) to ML_x. Early work[22] has demonstrated that the primary chemistry of HOOH is nucleophilic addition in matrices as weakly basic as water at pH 2. Hence, in the present systems with electrophilic metal complexes (ML_x), the initial step must be nucleophilic addition to the metal center, which also is true for the iron(II) center of aqueous Fenton chemistry[21]

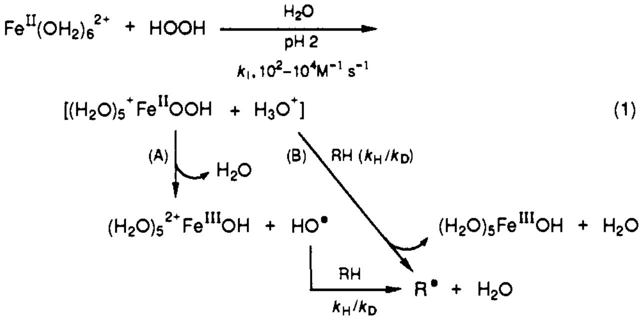

(1)

Although path A of eq 1 is the traditional formulation for the Fenton process, a recent study[23] provides compelling evidence that free hydroxyl radical is not the dominant reactant from highly stabilized iron(II) complexes [Fe^{II}(DETAPAC) and Fe^{II}(EDTA)], but rather the nucleophilic adduct reacts directly via path B of eq 1. Thus, for $Fe^{II}(OH_2)_6^{2+}$ and c-C_6H_{12} (RH), the apparent pathway is A and the k_H/k_D value is 1.1.[20]

For Fenton chemistry to occur via path A, the L_nFe^{III}–OH bond-formation energy ($-\Delta G_{BF}$) must be at least 51 kcal to induce the net rupture of the HO–OH bond (ΔH_{DBE}, 51 kcal mol^{-1}).[12] The redox potential for the $(H_2O)_6{}^{2+}Fe^{II}/(H_2O)_2{}^{2+}Fe^{III}$–OH couple is approximately +0.3 V vs NHE at pH 2, which is consistent with a $-\Delta G_{BF}$ value for Fe^{III}–OH of 53 kcal mol^{-1}.[24] For the present systems, the $Fe^{II}(PA)_2$ and $Fe^{II}(DPA)_2^{2-}$ complexes are the only ones to meet the bond-energetics limit, and both are highly stabilized iron(II) complexes [similar to Fe^{II}(DETAPAC) and Fe^{II}(EDTA)]. Hence, all of the complexes of this study must undergo nucleophilic addition by HOOH (or *t*-BuOOH) in a primary step to form an adduct that reacts with substrates via path B of eq 1.

Scheme IA outlines this process for the $Fe^{II}(PA)_2$/HOOH/c-C_6H_{12} system in $(py)_2HOAc$, which forms [$(PA)_2{}^{-}Fe^{II}OOH$ + pyH^+], **1**, in the primary step. The rate for the primary step is first-order in [$Fe^{II}(PA)_2$] and first-order in [HOOH], and the value of the apparent rate constant, k_1, is $(4 \pm 2) \times 10^3$ M^{-1} s^{-1} at room temperature.[2] A one-to-one combination of $Fe^{II}(PA)_2$ (19 mM) and HOOH (19 mM) in the presence of c-C_6H_{12} (1 M) reacts with 49% efficiency to give 6 mM c-C_6H_{11}py (apparently formed via path B of Scheme IA with a KIE of 1.7), 1 mM c-C_6H_{10}(O), and 1 mM $(c\text{-}C_6H_{11})_2$ (Table III, part A). (When 10 mM PhSeSePh is present, the reaction efficiency increases to 100% to give 17 mM c-C_6H_{11}SePh (via path B, Scheme IA) and 0.6 mM c-C_6H_{10}(O) and all of the iron is oxidized.) In contrast, for 3.3 mM $Fe^{II}(PA)_2$ and 56 mM HOOH, the reaction efficiency with 1 M c-C_6H_{12} is 72% to give 20 mM c-C_6H_{10}(O) and 1 mM c-C_6H_{11}OH (Table III, part A); for 5 mM $Fe^{II}(PA)_2$ and 100 mM HOOH, the reaction efficiency is 58% to give 27 mM c-C_6H_{10}(O) (KIE, 2.5) and 4 mM c-C_6H_{11}py (Table I, part A). Thus, the $Fe^{II}(PA)_2$/HOOH system (as well as all of the other catalysts of Table I) initially forms species **1** (Scheme IA), which reacts with (a) HOOH(Bu-t) via path A of Scheme I when it is present in excess and (b) c-C_6H_{12} via path B. For the 5 mM $Fe^{II}(PA)_2$/100 mM HOOH/1 M c-C_6H_{12} system, 96% of the HOOH

---

[20] (a) Rudakov, E. S.; Volkova, L. K.; Tret'yakov, V. P. *React. Kinet. Catal. Lett.* **1981**, *16*, 333–337. (b) Buxton, G. V.; Greenstock, C. L.; Helman, W. P.; Ross, A. B. *J. Phys. Chem. Ref. Data* **1988**, *17*, 513–886.

[21] Walling, C. *Acc. Chem. Res.* **1975**, *8*, 125–131.

[22] Halperin, J.; Taube, H. *J. Am. Chem. Soc.* **1952**, *74*, 380.

[23] Yamazaki, I.; Piette, L. H. *J. Am. Chem. Soc.* **1991**, *113*, 7588.

[24] Richert, S. A.; Tsang, P. K. S.; Sawyer, D. T. *Inorg. Chem.* **1989**, *28*, 2471.

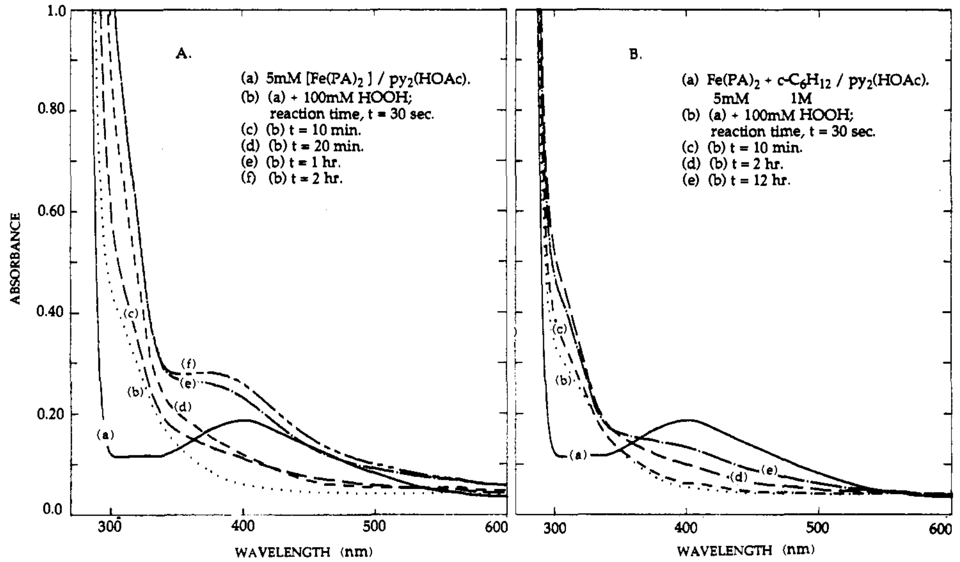

Figure 3. Absorption spectra in $(py)_2HOAc$ (A) for $Fe^{II}(PA)_2$ and for $Fe^{II}(PA)_2$ in the presence of excess HOOH at the indicated reaction times and (B) for $Fe^{II}(PA)_2$/1 M $c\text{-}C_6H_{12}$ alone and in the presence of excess HOOH at the indicated reaction times.

Scheme I. Activation of HOOH(Bu) by $Fe^{II}(PA)_2$ and of O_2 by $Fe^{II}(DPAH)(DPA)^-$ in $(py)_2HOAc$

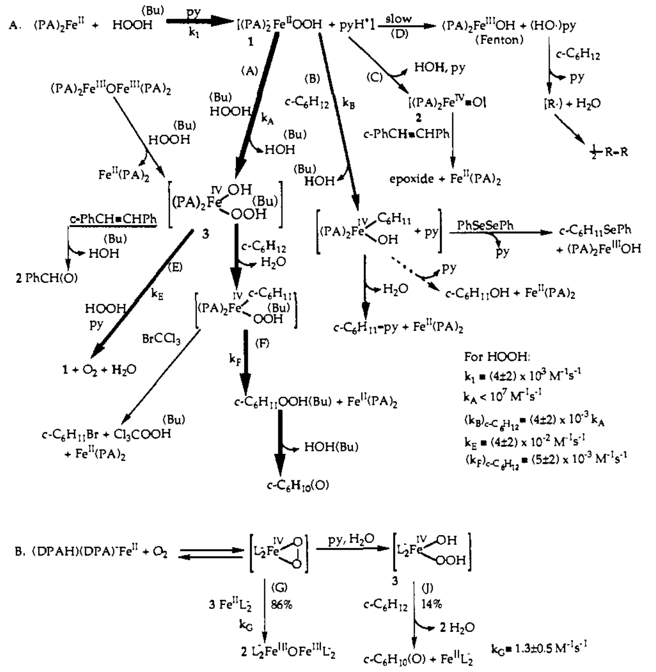

is consumed via path A and 4% via path B; with 3.3 mM $Fe^{II}(PA)_2$, 56 mM HOOH, and 1 M $c\text{-}C_6H_{12}$, 98% of the HOOH reacts via path A. Because the rate of disappearance of $Fe^{II}(PA)_2$ via reaction with HOOH is first-order in $[Fe^{II}(PA)_2]$ and first-order in [HOOH] (k_1, $(4 \pm 2) \times 10^3\ M^{-1}\ s^{-1}$) and reacts via path A, there is a stoichiometric factor of 2 for HOOH.

The hydroxylation of the aryl rings of $PhCH_3$ and $PhCH_2CH_3$ by the various species **1** (Table I, parts A and B) indicates that a hydroxyl group ($HO^\bullet$) is the reactive center [stabilized via a weak covalent bond (<15 kcal mol^{-1}) with the metal center] (free $HO^\bullet$ is 31 times more reactive with the aryl group than the methyl group of toluene).[20b] Species **1** is a precursor to hydroxyl radical ($HO^\bullet$) via path D of Scheme IA and as such should have a similar, but somewhat attenuated, reactivity [e.g., with $c\text{-}C_6H_{12}$ the KIE for $HO^\bullet$ is 1.1[20] and for species **1** is 1.7 [via path B to give $c\text{-}C_6H_{11}py$, Table III]]. Thus, the rate constants (k_B) for the reaction of species **1** with HOOH and with $c\text{-}C_6H_{12}$ should be smaller than those for $HO^\bullet$ (HOOH k, $2 \times 10^7\ M^{-1}\ s^{-1}$ and $c\text{-}C_6H_{12}$ k, $6 \times 10^9\ M^{-1}\ s^{-1}$)[20b] (a), and the relative rates of reaction for species **1** with HOOH and $c\text{-}C_6H_{12}$ are reversed (b) [for 5 mM $Fe^{II}(PA)_2$/100 mM HOOH/1 mM $c\text{-}C_6H_{12}$, rate(path A)/rate(path B) = 24 and k_A/k_B = 240 (Scheme IA)].

Both the electrochemistry (Figure 2) and the spectrophotometry (Figure 3) of the 5 mM $Fe^{II}(PA)_2$/100 mM HOOH system demonstrate that a new species (**3**, Scheme IA) is formed via the formation of species **1** in a rate-determining step [k_1, $(4 \pm 2) \times 10^3\ M^{-1}\ s^{-1}$], which rapidly reacts with a second HOOH. Electrochemical reduction of a freshly-formed solution is a multielectron catalytic cycle whereby the reduction product rapidly reacts with excess HOOH via path A to reform species **3** (at a scan rate of 0.01 V s^{-1}, 3 ECE cycles)

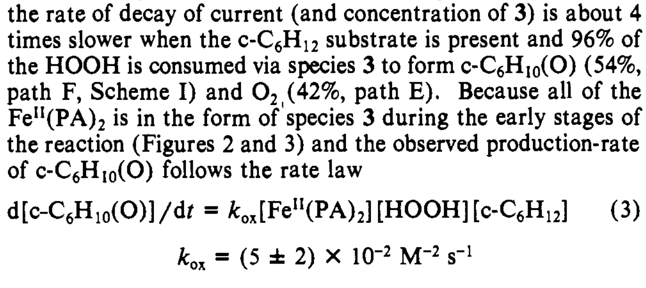

The presence of $c\text{-}C_6H_{12}$ does not affect the reduction of species **3** immediately after combination of the reagents (Figure 2), but the rate of decay of current (and concentration of **3**) is about 4 times slower when the $c\text{-}C_6H_{12}$ substrate is present and 96% of the HOOH is consumed via species **3** to form $c\text{-}C_6H_{10}(O)$ (54%, path F, Scheme I) and O_2 (42%, path E). Because all of the $Fe^{II}(PA)_2$ is in the form of species **3** during the early stages of the reaction (Figures 2 and 3) and the observed production-rate of $c\text{-}C_6H_{10}(O)$ follows the rate law

$$d[c\text{-}C_6H_{10}(O)]/dt = k_{ox}[Fe^{II}(PA)_2][HOOH][c\text{-}C_6H_{12}] \qquad (3)$$

$$k_{ox} = (5 \pm 2) \times 10^{-2}\ M^{-2}\ s^{-1}$$

reasonable rate expressions for paths F and E are as follows:

$$(F)\ d[c\text{-}C_6H_{10}(O)]/dt = k_F[\mathbf{3}][c\text{-}C_6H_{12}] \qquad (4)$$

$$k_F = (5 \pm 2) \times 10^{-3}\ M^{-1}\ s^{-1}$$

$$(E)\ d[O_2]/dt = k_E[\mathbf{3}][HOOH] \qquad (5)$$

$$k_E = (4 \pm 2) \times 10^{-2}\ M^{-1}\ s^{-1}$$

When *t*-BuOOH is used in place of HOOH, the results of Table II and the electrochemistry analogous to that of Figure 2 are consistent with the pathways of Scheme IA and the formation of reactive intermediates **1** and **3**. However, the rate of formation for species **3** and its reactivity with *t*-BuOOH and $c\text{-}C_6H_{12}$ are significantly changed (c-C_6H_{12} and HOOH, k_A/k_B = 240 and k_E/k_F = 8; c-C_6H_{12} and *t*-BuOOH, k_A/k_B = 19 and k_E/k_F = 15). Furthermore, with *t*-BuOOH the resultant species **3** reacts with methylenic carbons to produce ROOBu-*t* (via path F of Scheme IA) in addition to ketones. The ROOBu-*t* product is less favored than ROOH to undergo elimination of *t*-BuOH to give ketone ($-\Delta G_{BF}$ for *t*-BuO–H 97 kcal mol^{-1}, $-\Delta G_{BF}$ for HO–H 111 kcal mol^{-1}).[12,13] In the case of c-C_6H_{12}, the ratio of c-C_6H_{10}(O)/c-C_6H_{11}OOBu-*t* is 6:7 (13 mM total), but with $PhCH_2CH_3$ the ratio is 12:28 (40 mM total). Barton and co-workers[8] have detected the transient production of c-C_6H_{11}OOH from c-C_6H_{12} during the reaction life of a $Fe^{III}Cl_3$/HOOH/$(py)_4$HOAc system, but we have not observed any ROOH in the product solutions of Table I (probably because of the thermal instability of ROOH in the GC analytical protocols).

The $Fe^{II}(DPA)_2^{2-}$ complex in $(py)_2$HOAc is auto-oxidized by O_2 to give $(DPA)_2^{2-}Fe^{III}OFe^{III}(DPA)_2^{2-}$ (k_G, 1.3 M^{-1} s^{-1}; Scheme IB).[19] However, when hydrocarbon substrates are present, an intermediate of the auto-oxidation process transforms methylenic carbons to ketones (Table I, part A). Because the KIE values for this intermediate are the same as those for species **3** with c-C_6H_{12} and $PhCH_3$ (Table IA) and because the relative reactivity value {*R*} for $PhCH_2Me$/c-C_6H_{12} with this intermediate is the same (within experimental error) as for species **3**, a reasonable conclusion is that the two intermediates are functionally equivalent (Scheme IB). A closely similar species is formed from the combination of iron(II) porphyrin, O_2, and base [(Por)Fe^{II} + O_2 + HO^- $\rightarrow$ (Por)$Fe^{IV}(OH)(OO^-)$].[25]

Viability of Species 3 for Reaction with c-C_6H_{12}. The reduction potential for species **3** (eq 2, 0.0 V vs SCE, Figure 2) in relation to that for $(Cl_8TPP)Fe^{III}$–OH (−0.72 V vs SCE; $-\Delta G_{BF}$ = 31 kcal mol^{-1} for the Fe–OH bond)[24] provides a basis to estimate the energy of the Fe–OH bond in **3** ($-\Delta G_{BF}$, 15 kcal mol^{-1}). The energetics for the reaction of $HO^{\bullet}$ with $H^{\bullet}$ to form H–OH ($-\Delta G_{BF}$, 111 kcal mol^{-1})[13] is a measure of its reactivity with C–H bonds (ΔH_{DBE}(H_3C–H), 104 kcal mol^{-1}; $-CH_2$–H, 100 kcal mol^{-1}; >CH–H, 96 kcal mol^{-1}; ⋗C–H, 93 kcal mol^{-1}).[12] Hence, free $HO^{\bullet}$ reacts rapidly with all classes of C–H bonds.[20b] The extent to which the reactivity of $HO^{\bullet}$ that is bonded to iron is attenuated is related to its Fe–OH bond energy ($-\Delta G_{BF}$ = 15 kcal mol^{-1}). Thus, the $HO^{\bullet}$ in species **3** has an approximate reaction energy of 96 kcal mol^{-1} [$-\Delta G_{BF}$ = (111 − 15)]. This indicates that species **3** is able to abstract an H-atom from c-C_6H_{12} (ΔH_{DBE}, 95.5 kcal mol^{-1}) and methylenic carbons in general, but is not reactive with aliphatic methyl groups (RCH_3) or methane.

Likewise, the weaker the C–H bond energy of a methylenic group, the greater the reaction rate and efficiency for species **3**. This is confirmed for all of the complexes by the relative reactivity per >CH_2 group for $PhCH_2Me$ (ΔH_{DBE}, 85 kcal mol^{-1}) versus c-C_6H_{12} (ΔH_{DBE}, 95.5 kcal mol^{-1}) and is listed as {*R*} in Tables I and II; the values with HOOH range from 5.1 for $Fe^{II}(PA)_2$ to 26.5 for $Fe^{II}(MeCN)_4^{2+}$, and the values with *t*-BuOOH (a) to form ketone range from 2.3 for $Fe^{II}(OPPh_3)_4^{2+}$/MeCN to 14.6 for $Fe^{II}(OPPh_3)_4^{2+}/(MeCN)_4$py and (b) to form ROOBu-*t* range from 6.0 for $Fe^{III}Cl_3$/MeCN to 72 for $Co^{II}(bpy)_2^{2+}/(MeCN)_4$py. The kinetic isotope effect (KIE) values in Tables I and II for c-C_6H_{12} and $PhCH_3$ also are consistent with the formulation of species **3** with a weakly bonded $HO^{\bullet}$ as the primary reaction center. The variation in reactivity of **3** when formed from *t*-BuOOH rather than HOOH is illustrated by the results of Table IV for adamantane. The relative reaction probabilities to produce ketone via paths A–F are essentially the same. However, with *t*-BuOOH most of species **1** reacts with adamantane via path B of Scheme I.

The results in Table V for c-PhCH=CHPh are consistent with species **3** as the reactive intermediate for substrate dioxygenation. With the $Fe^{II}(DPA)_2^{2-}/O_2$ system the only product is via dioxygenation. However, under certain conditions the $Fe^{II}(PA)_2$/HOOH/$(py)_2$HOAc system produces epoxide (25% with 3.3 mM $Fe^{II}(PA)_2$/56 mM HOOH) either directly from species **1** or more probably by reaction with species **2** (that is formed via path C of Scheme IA).

Scheme II. Reactive Intermediates for Other ML_x Catalysts

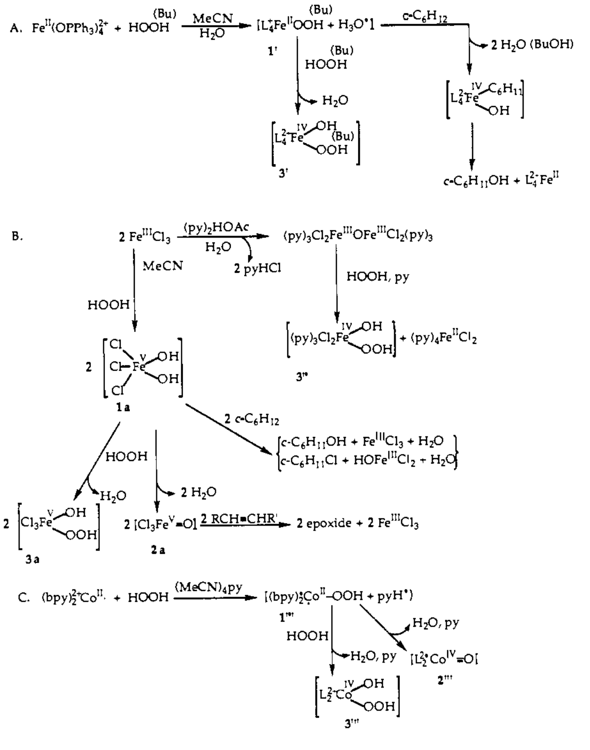

Reactive Intermediates for Other Catalyst Systems. The product profiles that are summarized in Tables I, II, and V indicate that the various ML_x/solvent systems must form reactive intermediates similar to those for $Fe^{II}(PA)_2/(py)_2$HOAc (**1**, **2**, and **3**). Thus, the $Fe^{II}(OPPh_3)_4^{2+}$/HOOH/MeCN system is not a viable Fenton reagent (iron(II/III) redox potential is too positive, +1.1 V vs SCE),[26] but produces significant amounts of alcohol from c-C_6H_{12} and other hydrocarbon substrates via direct reaction with species **1′** of Scheme IIA. This system also produces substantial yields of ketone via the competitive formation of species **3′** with excess HOOH.

Although some Gif systems[1,8,9] make use of $Fe^{III}Cl_3$ in py/HOAc media, reference to Table I indicates that the $Fe^{III}Cl_3$/MeCN system is much more efficient. The probable reaction path in $(py)_2$HOAc to form species **3″** is outlined in Scheme IIB. In contrast, with the absence of pyridine and H_2O, the $Fe^{III}Cl_3$ complex probably reacts with HOOH to form species **1a**, which reacts with c-C_6H_{12} to give equal amounts of c-C_6H_{11}OH and c-C_6H_{11}Cl (KIE, 2.9; Table I, part C)[6] and dehydrates to give species **2a** that epoxidizes olefins (Tables I and V).[6] Species **1a** reacts with excess HOOH to form species **3a**, which appears to have reactivities similar to species **3** and **3′** (Tables I, II, and V).

When 1:1 $Fe^{III}Cl_3$/HOOH (dry) is combined in anhydrous MeCN with olefins, epoxidation is the dominant, efficient process because formation of species **2a** (Scheme IIB) is favored in base-free matrices.[6] This species is an effective reaction mimic for compound I of horseradish peroxidase and of cytochrome P-450.[27] The presence of base (pyridine or H_2O) in the present systems favors hydrolysis of $Fe^{III}Cl_3$ to the *μ*-oxo dimer and subsequent formation of species **3″** via excess HOOH (Scheme IIB). However, it is likely that the various species **2a**, **2**, **2′**, and **2‴** are formed to a significant extent in the present systems (Scheme II and path C of Scheme IA) and that excess HOOH is the dominant competitive substrate to olefins (Tables I and V) to give species **3a**, **3**, **3′**, and **3‴**.

---

(25) Tsang, P. K. S.; Sawyer, D. T. *Inorg. Chem.* **1990**, *29*, 2848.

(26) Sawyer, D. T.; McDowell, M. S.; Spencer, L.; Tsang, P. K. S. *Inorg. Chem.* **1989**, *28*, 1166.

(27) Sugimoto, H.; Spencer, L.; Sawyer, D. T. *Proc. Natl. Acad. Sci. U.S.A.* **1987**, *84*, 1731.

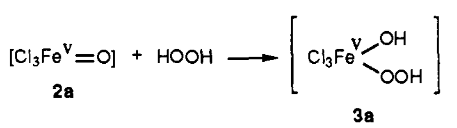

$$[\mathrm{Cl_3Fe^{V}{=}O}] + \mathrm{HOOH} \longrightarrow \left[\mathrm{Cl_3\overset{V}{Fe}}\begin{smallmatrix}\mathrm{OH}\\ \mathrm{OOH}\end{smallmatrix}\right] \qquad (6)$$

2a **3a**

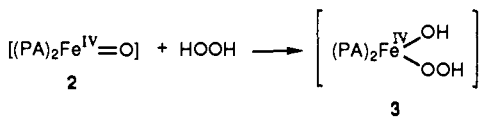

$$[\mathrm{(PA)_2Fe^{IV}{=}O}] + \mathrm{HOOH} \longrightarrow \left[\mathrm{(PA)_2\overset{IV}{Fe}}\begin{smallmatrix}\mathrm{OH}\\ \mathrm{OOH}\end{smallmatrix}\right] \qquad (7)$$

2 **3**

Species **2a** and **2** have chemical characteristics and reactivities (e.g., epoxidation of olefins, dehydrogenations, demethylation of *N*-methylaniline, and oxidative cleavage of α-diols) that are equivalent to those of Compounds I and II, respectively, of horseradish peroxidase and of ligninase.[7,27,28] In the reaction cycles of the latter,[28] a Compound III is formed via reaction of a second HOOH with Compound II, which is assumed to be $[\mathrm{(Por)Fe^{+}}](\mathrm{O_2}^{\bullet-})$. However, a more reasonable process is one that parallels that of eq 7 to give a product species that is similar to species **3** (Scheme IA)

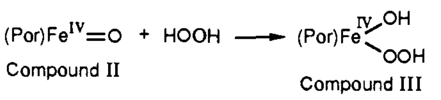

$$\mathrm{(Por)Fe^{IV}{=}O} + \mathrm{HOOH} \longrightarrow \mathrm{(Por)\overset{IV}{Fe}}\begin{smallmatrix}\mathrm{OH}\\ \mathrm{OOH}\end{smallmatrix} \qquad (8)$$

Compound II Compound III

The latter is equivalent to the protonated form of the product species from the combination of $\mathrm{(Cl_8TPP)Fe^{II}}$, $\mathrm{O_2}$, and $\mathrm{HO^-}$: $\mathrm{(Por)Fe^{IV}(OO^-)(OH)}$.[25]

The $\mathrm{Co^{II}(bpy)_2}^{2+}/\mathrm{HOOH/(MeCN)_4py}$ system is uniquely selective in the production of ketone from $c\text{-}\mathrm{C_6H_{12}}$, especially for larger concentrations (20 mM $\mathrm{Co^{II}(bpy)_2}^{2+}$/200 mM HOOH; Table I and Figure 1). The electrochemistry of this system indicates that a new oxidant ($E_{\mathrm{p,c}}$, 0.0 V vs SCE) is formed to a limited extent [~25% of the cobalt for 5 mM $\mathrm{Co^{II}(bpy)_2}^{2+}$/100 mM HOOH and ~42% for 20 mM/200 mM] and that its concentration correlates with the rate of production of ketone from $c\text{-}\mathrm{C_6H_{12}}$. These results indicate that a reactive intermediate is formed (**3‴**, Scheme IIC) via the initial limited formation of a $\mathrm{Co^{II}(bpy)_2}^{2+}$/HOOH adduct (**1‴**) and subsequent reaction with a second HOOH.

In summary, all of the systems in Tables I and II form (via nucleophilic addition) an ML_x/HOOH(Bu-*t*) adduct (species **1**, **1′**, **1a**, and **1‴**, Schemes I and II), which can react (a) directly with hydrocarbon substrates (RH) to give alcohols and/or Rpy derivatives (for pyridine-containing solvents) and (b) preferentially with excess HOOH(Bu-*t*) to give a reactive intermediate [$\mathrm{L}_x\mathrm{M(OH)(OOH)}$; species **3**, **3′**, **3a**, **3″**, and **3‴**, Schemes I and II] that selectively transforms methylenic carbons to ketones (and ROOBu-*t* when *t*-BuOOH is the oxidant). The KIE values for the reaction of the various species **1** (HOOH) with $c\text{-}\mathrm{C_6H_{12}}$ range from 1.7 [$\mathrm{Fe^{II}(PA)_2/(py)_2HOAc}$][29] to 2.9 [$\mathrm{Fe^{III}Cl_3}$/MeCN]. With *t*-BuOOH the KIE value for $\mathrm{Fe^{II}(PA)_2}$ is 4.6 and for $\mathrm{Fe^{III}Cl_3}$ is 5.8. Because all of the systems have KIE values that are significantly greater than that for free $\mathrm{HO^{\bullet}}$ (1.1),[20] the species **1** must include a hydroxyl group that is stabilized by weak bonding to oxygen or metal.

The apparent driving force for the monooxygenation of hydrocarbons by the various species **1** is the free energy of bond formation ($-\Delta G_{\mathrm{BF}}$) to give HO–H, plus the free energies of bond formation to give the $\mathrm{L}_x\mathrm{Fe^{IV}(OH)(R)}$ intermediate, minus the enthalpy for FeO–OH bond dissociation within species **1**. With each system HOOH(Bu-*t*) is a more reactive competitive substrate because the bond energy for HOO–H (ΔH_{DBE}, 89 kcal mol^{-1})[12] is much less than that for $c\text{-}\mathrm{C_6H_{12}}$ (ΔH_{DBE}, 95.5).[12] Likewise, the reactivity of HOOH(Bu-*t*) and RH with the various species **1** that are formed from *t*-BuOOH is much slower (KIE values are larger) because the bond energy of the *t*-BuO–H product (from H-atom abstraction of substrate: ΔH_{DBE}, 105 kcal mol^{-1}) is 14 kcal mol^{-1} less than that for the HOOH-formed species **1** (HO–H: ΔH_{DBE}, 119).

Similarly, the KIE values for the reaction of the various species **3** with $c\text{-}\mathrm{C_6H_{12}}$ to form $c\text{-}\mathrm{C_6H_{12}(O)}$ range from 2.5 for $\mathrm{Fe^{II}(PA)_2/(py)_2HOAc}$, $\mathrm{Fe^{II}(DPA)_2}^{2-}\mathrm{/(py)_2HOAc}$, and $\mathrm{Fe^{III}Cl_3/(py)_2HOAc}$ to >10 for $\mathrm{Fe^{III}Cl_3}$/MeCN, $\mathrm{Fe^{II}(OPPh_3)_4}^{2+}$/MeCN, and $\mathrm{Fe^{II}(MeCN)_4}^{2+}$/MeCN; with $\mathrm{PhCH_3}$ the KIE values are between 2.7 [$\mathrm{Fe^{II}(PA)_2}$] and 4.7 [$\mathrm{Fe^{II}(OPPh_3)_4}^{2+}$]. Substitution of *t*-BuOOH for HOOH gives the various species **3** that react with $c\text{-}\mathrm{C_6H_{12}}$ to form (a) $c\text{-}\mathrm{C_6H_{10}(O)}$ with KIE values between 7.6 and >10 and (b) $c\text{-}\mathrm{C_6H_{11}OOBu}$-*t* with KIE values between 5.4 and 8.7, and with $\mathrm{PhCH_3}$ to form (a) PhCH(O) (KIE values, 4.5 to >10) and (b) $\mathrm{PhCH_2OOBu}$-*t* (KIE values, 6.0 to >10). Again, the shifts to larger KIE values for *t*-BuOOH are consistent with the lower bond energetics for *t*-BuO–H formation relative to HO–H formation in reaction path F (Scheme IA). The same is true for the much longer life for $\mathrm{(PA)_2Fe^{IV}(OH)(OOBu}$-$t)$, **3**, and its much slower reactivity with *t*-BuOOH via path E of Scheme IA.

The species **3** for all of the systems except $\mathrm{Fe^{III}Cl_3/(MeCN)_4py}$ and $\mathrm{Co^{II}(bpy)_2}^{2+}$/MeCN have about the same reaction efficiency for the dioxygenation of c-PhCH=CHPh (Table V) when HOOH is the oxidant and are 10–95% less efficient with *t*-BuOOH. The $\mathrm{Fe^{III}Cl_3}$/MeCN system is exceptional because its reaction efficiency is 15% greater with *t*-BuOOH.

Consideration of the results of Tables I–V provides the basis to have the optimal system for the efficient and selective oxygenation of a specific hydrocarbon substrate. For example, the $\mathrm{Fe^{II}(OPPh_3)_4}^{2+}$/*t*-BuOOH/MeCN system is 68% efficient in its reaction with the allylic carbons of $c\text{-}\mathrm{C_6H_{10}}$ to give 95% $c\text{-}\mathrm{C_6H_9OOBu}$-*t* and 5% $c\text{-}\mathrm{C_6H_9OH}$, the $\mathrm{Fe^{II}(MeCN)_4}^{2+}$/HOOH/MeCN system ketonizes $\mathrm{PhCH_2Me}$ with 42% efficiency to give 92% PhC(O)Me and 8% $\mathrm{PhCH_2CH_2OH}$, and the $\mathrm{Fe^{III}Cl_3}$/*t*-BuOOH/MeCN system dioxygenates c-PhCH=CHPh with 53% efficiency to give 87% PhCH(O), 6% PhC(O)C(O)Ph, and 6% epoxide.

The present reactive intermediates (species **1**, **2**, and **3**) may be similar in form and function to those that are formed from the combination of HOOH with $\mathrm{Fe_2O(OAc)_2(bpy)_2Cl_2}$, $\mathrm{Fe_4O_2(OAc)_7(bpy)_2(ClO_4)}$, $\mathrm{Fe_2O(OAc)\{tris[(1\text{-}methylimidazol\text{-}2\text{-}yl)methyl]amine\}_2(ClO_4)_3}$, $\mathrm{Fe(ClO_4)_3{\cdot}6H_2O}$,[30] and $\mathrm{Fe_2[tris(2\text{-}pyridylmethyl)amine]_2O(ClO_4)_4}$.[31]

The formulations of **3**, **3′**, **3a**, **3″**, and **3‴** (Schemes I and II) as the reactive intermediates for the efficient and selective ketonization of methylenic carbons (e.g., $c\text{-}\mathrm{C_6H_{12}}$) meet the five criteria set forth in the introduction for an effective intermediate: (a) contains two available oxygen atoms; (b) does not produce alcohols as intermediates; (c) contains a reactive center ($\mathrm{HO^{\bullet}}$) that is able to break a 95.5 kcal mol^{-1} C–H bond; (d) formation of **3** is independent of the oxidation state of the iron complex; and (e) can be formed from $\mathrm{Fe^{II}(DPA)_2}^{2-}\mathrm{/O_2/(py)_2HOAc}$. Furthermore, the latter system transforms catechols to muconic acids (primarily as their anhydrides),[15] which is in accord with the formulation of species **3** (Scheme IB) as the reactive intermediate.

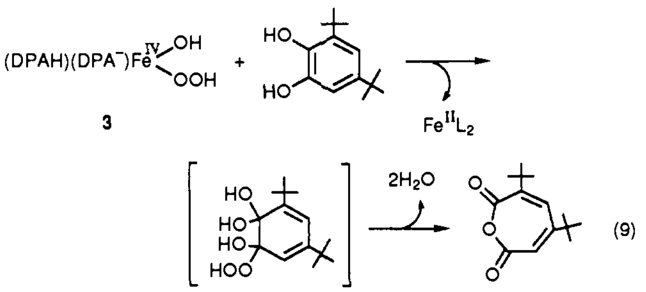

3 (9)

---

[28] Wariishi, H.; Marquez, L.; Dunford, H. B.; Gold, M. H. *J. Biol. Chem.* **1990**, *265*, 11137.

[29] Same value observed for $\mathrm{Fe^{II}(ClO_4)_2/(py)_4HOAc}$ by Barton, D. H. R.; Doller, D.; Geletii, Y. V. *Tetrahedron Lett.* **1991**, *31*, 3811.

[30] Fish, R. H.; Konings, M. S.; Oberhausen, K. J.; Fong, R. H.; Yu, W. M.; Christou, G.; Vincent, J. B.; Coggin, D. K.; Buchanan, R. M. *Inorg. Chem.* **1991**, *30*, 3002.

[31] Leising, R. A.; Brennan, B. A.; Que, L., Jr.; Fox, B. G.; Munck, E. *J. Am. Chem. Soc.* **1991**, *113*, 3988.

Related work in progress is directed to (a) the characterization of the reactivities of the various species **1**, **2**, and **3** with other functional groups (alcohols, amines, conjugated and nonconjugated polyolefins, thiols, ascorbic acid, α-tocopherol, and model substrates for lignin) and polyfunctional substrates, (b) the development of other ML_x/solvent systems for the selective formation of reactive intermediates **1**, **2**, and **3** (metals: Co, Cu, Mn, Cr, V, Mo, and Ru), and (c) the complete characterization of the various species **1**, **2**, and **3** by electrochemical, spectroscopic, magnetic, and kinetic measurements. Preliminary results indicate that (a) the $Fe^{II}(bpy)_2^{2+}$/HOOH/py system is an effective reaction mimic (via production of species **1**) for ligninase (selectively dehydrogenates $3,4\text{-}(MeO)_2PhOH)$[32,33] and (b) several $Cu^{II}L_x$ complexes activate HOOH in a manner similar to that of $Co^{II}(bpy)_2^{2+}$.[3]

Acknowledgment. This work was supported by the National Science Foundation under Grant No. CHE-9106742, the Welch Foundation under Grant No. 1042A, and the State of Texas under the Texas Advanced Research Program. We are grateful to Professor D. H. R. Barton (of this department) for making available preprints of related investigations and for his assistance, encouragement, and stimulating discussions.

Registry No. $Fe^{II}(PA)_2$, 46940-39-0; $Fe^{II}(DPA)_2^{2-}$, 71605-20-4; $Fe^{III}Cl_3$, 7705-08-0; $[Fe^{II}(O_2bpy)_2](ClO_4)_2$, 139657-03-7; $[Fe^{II}(OPPh_3)_4](ClO_4)_2$, 28959-14-0; $[Fe^{II}(MeCN)_4](ClO_4)_2$, 97690-72-7; $[Fe^{II}(bpy)_2](ClO_4)_2$, 16581-25-2; $[Co^{II}(bpy)_2](ClO_4)_2$, 78624-86-9; $[Fe^{II}(H_2O)_6](ClO_4)_2$, 15305-57-4; $[Co^{II}(MeCN)_4](ClO_4)_2$, 139657-04-8; HOOH, 7722-84-1; *t*-BuOOH, 75-91-2; $c\text{-}C_6H_{12}$, 110-82-7; $PhCH_2CH_3$, 108-88-3; $c\text{-}C_6H_{10}$, 110-83-8; *cis*-PhCH=CHPh, 645-49-8; D_2, 7782-39-0; $(Me_4N)PA$, 139657-01-5; $(Me_4N)_2DPA$, 124443-96-5; PAH, 98-98-6; $DPAH_2$, 499-83-2; $bpyO_2$, 7275-43-6; bpy, 366-18-7; $C_{10}H_{16}$, 281-23-2; $C_6H_{10}(O)$, 108-94-1; $C_6H_{11}py$, 15787-49-2; $PhC(O)CH_3$, 98-86-2; $PhCH(OH)CH_3$, 98-85-1; $HOPhCH_2CH_3$, 25429-37-2; PhCH(O), 100-52-7; $HOPhCH_3$, 1319-77-3; $C_6H_8(O)$, 25512-62-3; $C36H_9OH$, 25512-63-4; $c\text{-}C_6H_{10}$ epoxide, 286-20-4; $c\text{-}C_6H_{11}OOBu\text{-}t$, 15619-54-2; $c\text{-}C_6H_{11}OH$, 108-93-0; $PhCH(OOBu\text{-}t)CH_3$, 28047-94-1; $PhCH_2OOBu\text{-}t$, 18774-10-2; PhSeSePh, 1666-13-3; *m*-ClPhC(O)OOH, 937-14-4; PhC(O)C(O)Ph, 134-81-6; $(c\text{-}C_6H_{11})_2$, 92-51-3; $PhSe(c\text{-}C_6H_{11})$, 22233-91-6; PhSe(py), 87803-47-2; $C_{10}H_{14}(O)$, 700-58-3; $1\text{-}C_{10}H_{15}O$, 768-95-6; $1\text{-}C_{10}H_{15}\text{-}2\text{-}py$, 29768-05-6; $1\text{-}C_{10}H_{15}\text{-}4\text{-}py$, 60159-38-8; *cis*-PhCH=CHPh epoxide, 1689-71-0; $PhCH_2CH_2OH$, 60-12-8; $PhCH_2OH$, 100-51-6.

---

(32) Schmidt, H. W. H.; Haemmerli, S. D.; Schoemaker, H. E.; Leisola, M. S. A. *Biochemistry* **1989**, *28*, 1776.

(33) Tung, H.-C.; Sawyer, D. T. *Biochemistry*, submitted for publication.

The Surface Nature of Grignard Reagent Formation[1]

H. M. Walborsky* and Marek Topolski

Contribution from the Dittmer Laboratories of Chemistry, Florida State University, Tallahassee, Florida 32306. *Received November 20, 1991*

Abstract: The reaction of *exo*-2-norbornyl bromide with Rieke magnesium in ether at −70 °C in the presence of *tert*-butyl alcohol-*O-d* gave exclusively *exo*-2-deuterionorbornane whereas the epimer *endo*-2-norbornyl bromide yielded a 1:1 mixture of *endo*- and *exo*-2-deuterionorbornane. Reaction of the epimeric bromides with Rieke magnesium in the presence of *tert*-butyl alcohol and a 10-fold equivalent excess of the radical trap deuterated dicyclohexylphosphine resulted in only 8% deuterium incorporation in the products. Treatment of *exo*-5-bromo-2-norbornene under identical conditions (*tert*-butyl alcohol-*O-d*, −70 °C) yielded a 65:35 mixture of *exo*-5-deuterio-2-norbornene and 3-deuterionortricyclene. In the presence of *tert*-butyl alcohol and a 10-fold excess of deuterated dicyclohexylphosphine the reaction of *exo*-5-norbornenyl bromide gave the same mixture of products but with only 8% deuterium incorporated. These results strongly support the surface nature of the Grignard formation reaction.

Introduction

In 1964, on the basis of experimental evidence involving stereochemical studies as well as analyses of products, we proposed our initial mechanism for Grignard reagent formation.[2c] This mechanism was elaborated[2e] upon in 1973 and is depicted in Scheme I. There is general agreement that the reaction is initiated by an electron transfer from the magnesium surface to the σ^* antibonding orbital of the carbon–halogen bond (outer sphere, pathway 1) to produce a tight radical anion–radical cation pair and that this is the rate-determining step of the reaction.[2-8] There is also agreement that free radicals are involved in this reaction, formed either directly by inner-sphere electron transfer from the

Scheme I. Proposed Mechanism for Grignard Reagent Formation

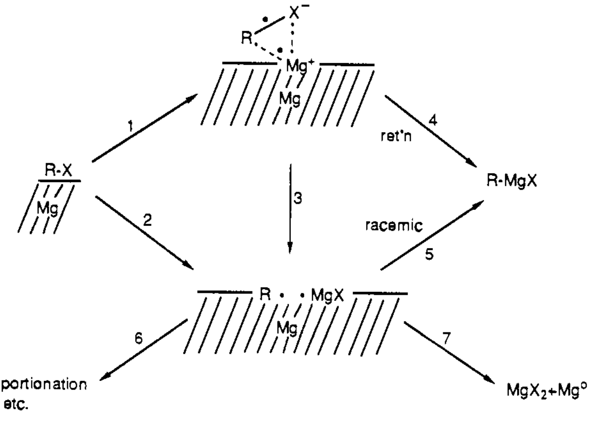

---

[1] This work was supported by a grant from the National Science Foundation, to whom we are grateful.

[2] (a) Walborsky, H. M.; Young, A. E. *J. Am. Chem. Soc.* **1961**, *83*, 2595. (b) Walborsky, H. M. *Rec. Chem. Prog.* **1962**, *23*, 75. (c) Walborsky, H. M.; Young, A. E. *J. Am. Chem. Soc.* **1964**, *86*, 3288. (d) Idem. *Baskerville Chem. J.* **1965**, *14*, 1. (e) Walborsky, H. M.; Aronoff, M. S. *J. Organomet. Chem.* **1973**, *51*, 33. (f) Walborsky, H. M.; Banks, R. B. *Bull. Soc. Chim. Belg.* **1980**, *89*, 849. (g) Walborsky, H. M. *Tetrahedron* **1981**, *37*, 1625. (h) Boche, G.; Walborsky, H. M. In *The Chemistry of the Cyclopropyl Group*; Rappoport, Z., Ed.; John Wiley & Sons Ltd.: London, 1987; Chapter 12. (i) Walborsky, H. M.; Rachon, J. *J. Am. Chem. Soc.* **1989**, *111*, 1896. (j) Rachon, J.; Walborsky, H. M. *Tetrahedron Lett.* **1989**, *30*, 7345. (k) Boche, G.; Walborsky, H. M. *Cyclopropane Derived Reactive Intermediates*; John Wiley & Sons: London, 1990. (l) Walborsky, H. M. *Acc. Chem. Res.* **1990**, *23*, 286. (m) Walborsky, H. M. *Chem. Unserer Zeit* **1991**, *25*, 108.

[3] (a) Kharasch, M. S.; Reinmuth, O. *Grignard Reactions of Non-Metallic Substances*; Prentice-Hall: New York, 1954. (b) Gomberg, M.; Bachman, W. E. *J. Am. Chem. Soc.* **1927**, *49*, 236.

0002-7863/92/1514-3455$03.00/0